to the family of *N*-acylethanolamines that are generated by the enzyme *N*-acylphosphatidylethanolamine-hydrolyzing phospholipase D. The anandamide (AEA) and 2-AG, the first lipids identified to have orexigenic activities, are the main endogenous agonists of cannabinoid receptors found in the brain and other tissues associated with orexigenic effects (Pagotto and Pasquali, 2005; Engeli et al., 2005; Howlett et al., 2002). In contrast, some other anorectic lipid classes of structurally-related compounds, such as *N*-palmitoylethanolamine (PEA), *N*-oleoylethanolamine (OEA) and *N*-stearoylethanolamine (SEA), have been reported to be involved in the anorectic response (Terrazzino et al., 2004; Schmid et al., 2002).

In light of recent progress in understanding the regulation of eating behavior in the central nervous system, it is interesting to investigate the effects of OOS-TMP on the peripheral *N*-acylethanolamines levels in the gastrointestinal tract. Thus, one of the aims of the present study was to determine the levels of peripheral *N*-acylethanolamines including PEA, OEA, SEA, AEA, 2-AG that are closely associated with appetitive function, lipid homeostasis, behavior and energy balance in mice treated with OOS-TMP. In the present study, we used C57BL/6J (B6) mice, which are genetically more homogenous than ddY mice, which were not derived from an inbred mouse strain.

ins2$^{+/Akita}$ mice, a model of type 2 diabetes (Yoshioka et al., 1997), carries a C96Y mutation in the Ins2 gene on a B6 background (Wang et al., 1999). While B6-*lepr*^{db}/*lepr*^{db} (db/db) mice, a well-established genetic rodent model of hyperphagia, obesity, insulin resistance, is another model of type 2 diabetes (Hummel et al., 1966; Shao et al., 2000). As both of these diabetic models are characterized by hyperglycemia and hyperphagia, we intended to explore whether or not OOS-TMP has an influence in these mice.

2. Methods

2.1. Animals

The study protocol was approved by the Animal Research Committee of Kyoto University. All mice were handled in accordance with the Animal Welfare Guidelines of Kyoto University. We used male mice throughout this study. We purchased B6 and B6 background db/db and diabetic nonobese Akita mice(*ins2*$^{+/Akita}$) from Japan SLC, Inc. (Shizuoka, Japan). A total of 45 mice were housed individually and given free access to a pelletized chow and water during the acclimatization period, except when otherwise indicated. A standard commercial lab chow diet (F-2, 3.73 kcal/g, Funahashi Farm Corp., Chiba, Japan) was used. All animals were maintained at an ambient temperature of 24±2 °C and 50±10% humidity with a 12 h dark–light cycle (lights on at 7:00 AM).

2.2. Chemicals and OOS-TMP

All chemicals were of the purest analytical grade. OOS-TMP was synthesized and purified as previously described by Hasegawa and Koizumi (1990). The purity of the compound was found to be more than 99.8% as determined by NMR (JEOL JNM-EX400KS, JEOL Ltd. Akishima, Tokyo, Japan). PEA, OEA, AEA, 2-AG and SEA were purchased from Cayman Chemical Co. (Ann Arbor, MI).

2.3. i.c.v. cannulation

The surgical operation for i.c.v. cannulation was carried out as reported by Asakawa et al. (2001). Briefly, mice were anesthetized with sodium pentobarbital by i.p. injection (80–85 mg/kg) and fixed in a stereotaxic frame (SR-6, Narishige, Tokyo, Japan). A small hole was made in the skull using a needle inserted 0.9 mm lateral to the central suture and 0.9 mm posterior to the bregma. A 24-gauge cannula beveled at one end over a distance of 3 mm (Safelet-Cas, Nipro, Osaka, Japan) was put into the third cerebral ventricle for i.c.v. injection. The stainless-steel cannula was fixed to the skull with dental cement and capped with silicon without an obtruder. The animals were allowed to recover for 1 week before any experimental manipulation.

To ascertain the injection site that the drugs were injected exactly into the cerebral ventricle, at the end of all i.c.v. experiments, diluted India ink was injected through the cannula and animals were killed immediately by anesthetic overdose. Only those animals showing uniform distribution of ink into the ventricles were used for statistical analysis.

2.4. i.c.v. injection and experimental process

Conscious 7-week old animals were gently restrained by hand. A dose of 5 mg/kg of OOS-TMP was chosen because this dose induced hypophagia by upregulating of CRF without any toxicological signs (Huang et al., 2007). Four microliters of various concentrations of OOS-TMP dissolved in 5% dimethylsulfoxide (DMSO) in 0.9% saline were injected i.c.v. using a microsyringe via PE-20 tubing fitted with a 27-gauge needle that was inserted through the guide cannula to a depth of 3 mm below the external surface of the skull. Control animals received an equivalent volume of vehicle (5% DMSO in 0.9% saline). Before feeding tests, mice were fasted for 16 h with unlimited access to water. OOS-TMP or vehicle was singly administered by i.c.v. to food-deprived mice at 10:00 a.m. Food intake was recorded at 20 min and at 1, 2, 4, 6 and 24 h, and body weights were monitored at 0, 6, 12 and 24 h after i.c.v. injection. To determine the blood glucose levels, blood samples were collected from the tail vein immediately before fasting at between 18:00 and 19:00 pm, and a further sample was obtained from the orbital sinus at 10:00 am, i.e., 24 h after i.c.v. injection. The blood glucose levels were determined using a glucometer (Glutest Ace; Arkray Factory, Shiga, Japan), which used the glucose oxidase method. At the end of observation, mice were sacrificed by rapid decapitation. The intestines were removed quickly, rinsed with 2×1 ml ice-cold saline, and then immediately stored in liquid nitrogen at −70 °C until analyzed. In addition, we obtained and stored the lung to investigate lung injury.

2.5. Gas chromatography/mass spectrometer (GC/MS) analysis of N-acylethanolamines in the intestine

The intestinal content of *N*-acylethanolamines was determined by isotope-dilution GC/MS (Giuffrida and Piomelli, 1998; Felder et al., 1996). Lipid extraction and fractionation were performed as previously described (Schmid et al., 1995; Yang and Karoum, 1999) with a slight modification. Thawed intestine (0.6 g) was homogenized in 20 ml chloroform and spiked with an isotope mixture (5 μl) containing ^{13}C labeled 2-AG, AEA, PEA, SEA and OEA (500 pmol each) as internal standards. Then, 10 ml of 0.5% saline and 10 ml of methanol were added, shaken for 1 h and centrifuged at 15,000 ×g for 15 min. The lipid chloroform fraction was recovered; a further 10 ml of 0.5% saline and 10 ml methanol was added, and the mixture incubated for another 20 min and centrifuged as described above. This step was repeated twice. The lipid chloroform fraction was dried on a rotary evaporator at a temperature below 50 °C. The lipid extract was redissolved in 5 ml of chloroform and applied to a column (Presep-C Florisil, Wako Pure Chemical Industries. Ltd., Osaka, Japan). The lipid extracts were washed with hexane, 0.1% acetic acid in hexane and then 20% ethyl acetate in hexane, and eluted using 2% methanol in chloroform. The fractions eluted in 2% methanol in chloroform were collected and dried with a stream of nitrogen. The dried residues were derivatized by adding100 μL O-Bis(trimethylsilyl)trifluoroacetamide. The vials were tightly capped and heated at 50 °C for 60 min. After cooling to room temperature, the derivatives were dried under nitrogen, reconstituted in 50 μL of chloroform and vortex mixed. The extracts were injected into an Agilent Technologies 6890 N Network GC equipped with an HP-5MS column (30 m×0.25 mm i.d., Hewlett-

Table 1
Effects of a single i.c.v. injection of OOS-TMP (5 mg/kg) on gut lipids (B6)

Time after dosing		Number of mice	Anrexigenic lipids (pmol/g tissue)			Orexigenic lipids (pmol/g tissue)	
			PEA	OEA	SEA	AEA	2AG
2 h	Case	5	63.61±19.59	1.11±1.56	37.85±7.02 *	7.38±0.87	1719.58±599.69
	Controls	5	59.73±11.09	0.74±0.73	52.99±9.00	6.1±0.88	1290.49±119.90
24 h	Case	5	184.93±35.16	85.4622±89.83	13.362±4.97	0.497±0.59	3565.74±1164.00 *
	Control	5	232.83±68.56	200.43±103.35	12.41±5.05	0.93±0.92	1698.21±450.79

n=5 per group *p<0.05 vs. control.
*Significant (p<0.05).

Packard, Palo Alto, CA) in the splitless mode. Mass spectral data were acquired using the Agilent 5973 Network Mass Selective Detector. The oven temperature was increased from 150 °C to 280 °C at a rate of 10 °C per min. The M-15 ions were monitored using the selected ion monitoring mode.

2.6. Statistical analysis

For the levels of *N*-acylethanolamines, statistical analysis was performed using the Wilcoxon signed-rank test. One-way analysis of variance (ANOVA) was used for the cumulative food intake, relative body weight, and blood glucose level. When ANOVA was significant, the Duncan procedure was performed for multiple comparisons, All analyses were done using STATISTICA™ software (StatSoft®, Japan). A p value<0.05 was considered to be significant.

3. Results

3.1. Effects of a single i.c.v. injection of OOS-TMP on the levels of N-acylethanolamines in the intestine of B6 mice at 2 h and 24 h

Previous studies have shown that anorexia generated by OOS-TMP is partly mediated by its action on the central nervous system, while the profile of the peripheral gastrointestinal system is currently unclear. Therefore, we determined the levels of *N*-acylethanolamines (NEAs) including PEA, OEA, SEA. AEA, 2-AG fatty acid amide compounds in intestines (peripheral organ) to investigate whether OOS-TMP acts on the gastrointestinal system resulting in anorexia, hypopraxia.

We determined the levels of *N*-acylethanolamines (NEAs) in the intestines at 2 h and 24 h after administration of OOS-TMP. As shown in Table 1, at 2 h, quantification of NEAs by GC/MS revealed that that the level of SEA, an anorexic lipid mediator, was significantly decreased after treatment with OOS-TMP at a dose of 5 mg/kg compared with the control group, while its congeners, the other two types of orexic lipid mediators AEA and 2-AG, were slightly increased. On the other hand, at 24 h, the level of 2-AG, an orexigenic lipid mediator, was further increased (Table 1), while the levels of PEA and OEA, an anorexic molecule, declined to a lesser extent. No detectable changes were observed in SEA compared with the controls (Table 1).

The present results indicated that the orexigenic profile of the endocannabinoid levels was strengthened in the intestine with OOS-TMP at a dose of 5 mg/kg at 2 h and 24 h albeit with significant anorexia.

3.2. Effects of OOS-TMP on cumulative food intake, body weight gain and blood glucose in B6, Akita and db/db mice

Next, we investigated whether OOS-TMP induces comparable anorexigenic effects in the hyperphagic mouse models Akita and db/db mice. OOS-TMP significantly inhibited feeding in B6 at all time points, while feeding in the Akita and db/db mice had recovered somewhat by 4 h, indicating that the effects of OOS-TMP were less intensive in these hyperphagic mice. However, of interest is that at 24 h, OOS-TMP significantly inhibited food intake in these mice (OOS-TMP vs control (g); B6 mice: 0.28±0.4 vs 4.55±1.54; Akita: 1.02±0.45 vs 3.38±0.65; db/db:1.85±0.21 vs 5.35±0.86; Fig. 1A, B, C). It should be also pointed out that food consumption by Akita mice and db/db mice did not showed hyperphagia when compared with controls. However, the cumulative food consumption at 24 h in treated mice was significantly larger in Akita or db/db than in C57BL/6 (p<0.05).

After administration of OOS-TMP, mice displayed weight loss and decreased food intake. In particular, from 12 to 24 h a significant body weight reduction was observed in Akita mice, and db/db mice showed significant body weight loss at 24 h (p<0.001). The mean and SD of

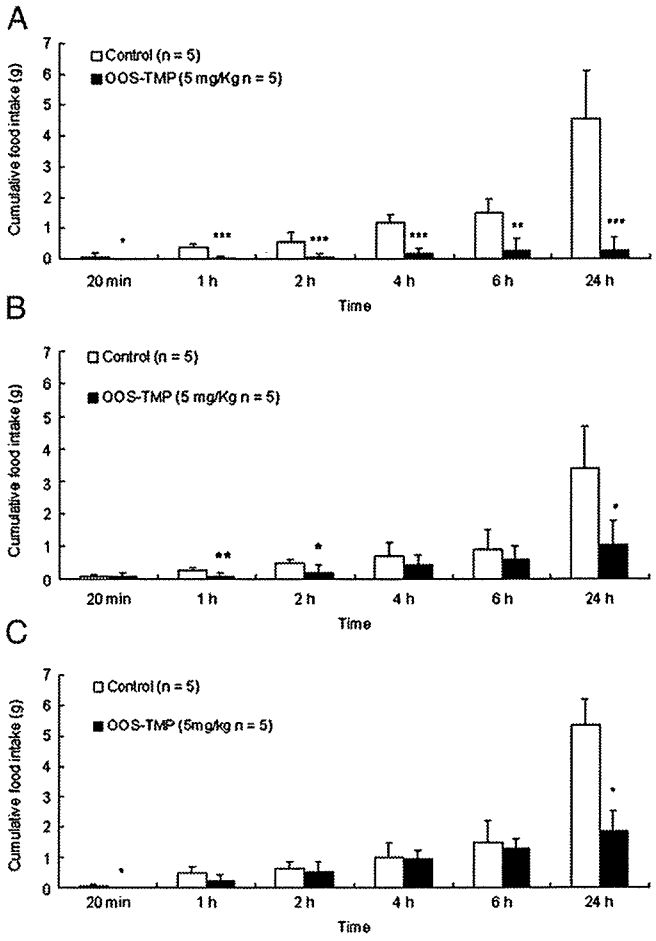

Fig. 1. Effects of a single i.c.v. injection of OOS-TMP (5 mg/kg) on cumulative food intake in B6, Akita and db/db mice from 20 min to 24 h. A. Effect of OOS-TMP on cumulative food intake in food-deprived B6 mice. n=5; *p<0.05 *vs.* control, **p<0.01 *vs.* control, ***p<0.001 *vs.* control; B. Effect of OOS-TMP on cumulative food intake in food-deprived Akita mice. n=5; *p<0.05 *vs.* control, **p<0.01 *vs.* control, ***p<0.001 *vs.* control; C. Effect of OOS-TMP on cumulative food intake in food-deprived db/db mice n=5; *p<0.05 *vs.* control, **p<0.01 *vs.* control, ***p<0.001 *vs.* control.

body weight (g) at 24 h were 23.4±2.25 for B6 mice, 19.98±0.99 for Akita mice and 44.97±1.00 for db/db mice (Fig. 2A,B,C).

Histological examination of the lungs form these mice revealed mild desquamation of the Clara cells in the bronchi as previously reported in ddY mice (Huang et al., 2007) and an absence of alveolar damage at 24 h (data not shown).

Blood glucose levels were significantly decreased at 24 h after OOS-TMP administration in Akita mice (n=5); 414.00±96.71 mg/dL before treatment and 138.00±139.40 mg/dL at 24 h after treatment (p<0.01). In contrast, blood glucose levels in Akita mice without treatment (n=5) were (509.00±90.21 mg/dL) before vehicle treatment and (538.75±70.74 mg/dL) at 24 h after vehicle treatment. In db/db mice, blood glucose levels were (n=5); 258.20±74.16 mg/dL before treatment and 347.60±108.34 mg/dL at 24 h after dosing (p>0.05) while in db/db control mice, they were (277.75±111.33 mg/dL) and (407.25±157.31 mg/dL) respectively (p>0.05).

4. Discussion

Appetite and energy homeostasis are regulated by various stimulatory (orexigenic) and inhibitory (anorexigenic) signaling pathways involving the central nervous system and the gastrointestinal system. Our previous study demonstrated that OOS-TMP induced anorexia, hypopraxia and enhanced the expression of corticotropin releasing factor (CRF), anorexigenic signalling, in the hypothalamus without apparent toxicity (Huang et al., 2007). However, the effects of *N*-acylethanolamines on the intestine have not been investigated. In this paper, sensitive and specific GC/MS assay was used to determine changes in intestinal levels of *N*-acylethanolamines, including PEA, OEA, SEA, AEA and 2-AG.

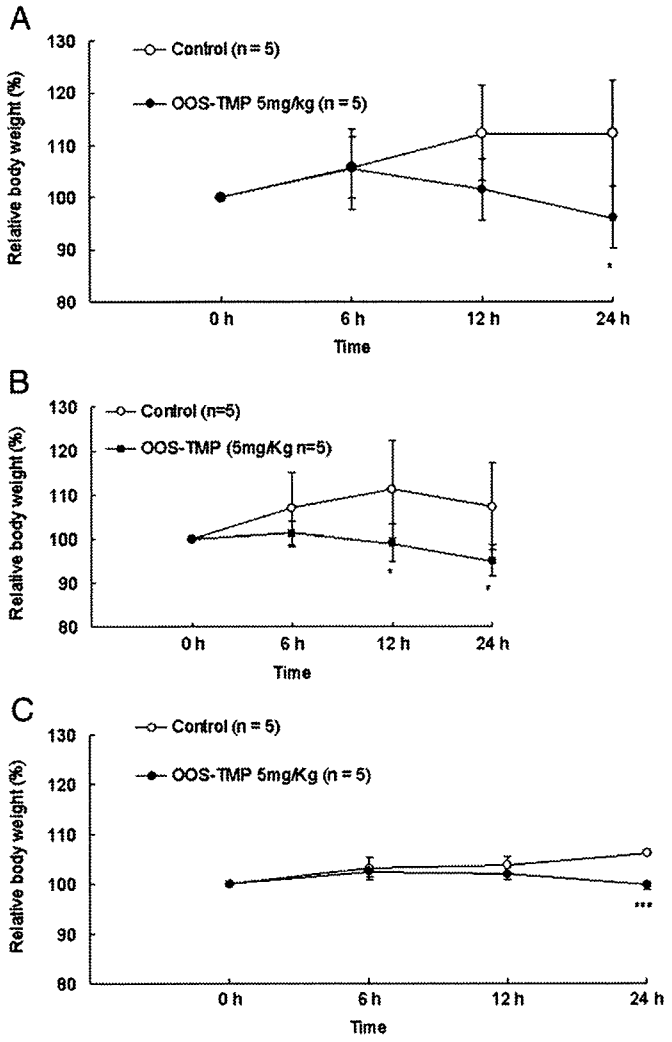

Fig. 2. Effects of a single i.c.v. injection of OOS-TMP (5 mg/kg) on relative body weight of B6 mice, Akita mice and db/db mice from 0 to 24 h. A. Effect of OOS-TMP on relative body weight in food-deprived *B6* mice. n=5; *p<0.05 *vs.* control, **p<0.01 *vs.* control, ***p<0.001 *vs.* control; B. Effect of OOS-TMP on relative body weight in food-deprived Akita mice. n=5*p<0.05 *vs.* control, **p<0.01 *vs.* control, ***p<0.001 *vs.* control; C. Effect of OOS-TMP on relative body weight in food-deprived db/db mice. n=5; *p<0.05 *vs.* control, **p<0.01 *vs.* control, ***p<0.001 *vs.* control.

It appears that *N*-acylethanolamines signalling via cannabinoid receptors modulates food intake, lipid homeostasis, behaviour and energy balance (Pacher et al., 2006; Cota et al., 2003; Kirkham et al., 2002; Onaivi et al., 2002). Endocannabinoids are implicated in appetite and body weight regulation. 2-AG was the first endocannabinoids to be identified, and is the arachidonate ester of glycerol, which activates both the CB_1 and CB_2 receptors (Mechoulam et al., 1995; Sugiura et al., 1995). Surprisingly, the present study revealed an orexigenic pattern in the intestine at both 2 h and 24 h. Importantly, 2-AG levels remained constantly higher than control at 2 and 24 h conditions, especially, at 24 h, with twofold increase in mice small intestines.

Recently, it has been suggested that 2-AG reduces spontaneous locomotor activity and rearing frequency in a dose-dependent manner (Darmani, 2002). Other studies in rodents have also shown that larger doses of 2-AG and AEA are motor suppressive and both compounds are equipotent in reducing spontaneous locomotor activity (Mechoulam et al., 1995). The present study confirmed that the reduction in locomotor activity requires larger doses of 2-AG as the 2-AG level was1719.58±599.69 pmol/g at 2 h with mice exhibited low locomotor activity and the level at 24 h was 3565.74±1164.00 pmol/g and the mice displayed typical hypopraxia. Given that one of important finding of the present investigation is that the high concentration of 2-AG may be responsible for the reduction in locomotor activity observed, there are two contradictory statuses, in that there was anorexigenic dominance in the central nervous system and orexigenic dominance in the gastrointestinal system. Taken together, it can be concluded that anorexigenic signals in the central nervous system may predominate eating behaviour. By contrast, the endocannabinoid system in the gastrointestinal system may be involved in the locomotor suppression reduced by OOS-TMP.

N-stearoylethanolamine (SEA) has recently been reported also to inhibit food intake by downregulating of liver gene expression of stearoyl-coenzyme A desaturase 1, while PPARα, PPARβ, and PPARγ expression was unaffected (Terrazzino et al., 2004). In the present study, however, we observed an orexigenic profile with significantly declined amount of SEA in intestines at 2 h but unchanged at 24 h after OOS-TMP treatment.

The possible physiological and pathological significance of the changes of *N*-acylethanolamines in the feeding-associated brain region including the hypothalamus, brain stem and limbic forebrain remains to be determined in the future. Particularly, the 2-AG level in the brain needs to be determined because it is found in both the gastrointestinal tract and the brain (Mechoulam et al., 1995).

The present study confirms the previously reported anorexigenic effect of OOS-TMP (Huang et al., 2007; Hasegawa and Koizumi, 1990; Koizumi et al., 1988). However, there are subtle inconsistencies: B6 control mice continued to be hypophagic at 24 h while early recovery in eating behavior was observed in ddY mice (Huang et al., 2007). This discrepancy may indicate a genetic difference in susceptibility to OOS-TMP between these two widely used mice strians. In fact, B6 mice are more genetically homogeneous than ddY mice. Another inconsistency may be related to the absence of hyperphagia in the Akita and db/db control mice that underwent i.c.v. surgery, but without administration of OOS-TMP, when compared with their counterpart control mice. This may be associated with susceptibility to surgery: Akita and db/db might be more susceptible to the damage associated with i.c.v.

surgery. However, when these three types of mice were compared at the 24 h timepoint, the Akita and db/db mice treated with OOS-TMP consumed more diet than the B6 mice ($p<0.05$). Therefore, these results are consistent with our previous observation in that the anorexigenic effects of OOS-TMP in hyperphagic mice, Akita (Toyoshima et al., 2007) and db/db mice were ameliorated compared with wild-type B6 mice.

In our experiment, there was a striking drop in blood glucose in the Akita diabetic mice and a loss of body weight at 24 h, the db/db, Akita and B6 mice after i.c.v. administration of OOS-TMP. This observation suggests that OOS-TMP may have potential anti-obesity and anti-diabetic-like effects in a variety of animal models of eating-related disorders. Comprehensive understanding of the molecular and biochemical mechanism of OOS-TMP-induced anorexia warrants further exploration.

In summary, the present data indicate that peripherally NEAs are not involved in the hypophagia but instead hypopraxia caused by OOS-TMP. We have also shown that the endocannabinoid 2-AG is the most sensitive to variation during feeding. Overall, these findings are consistent with previous reports and support the role of endocannabinoids in the physiological regulation of appetite, body weight and behavior control. Although we observed changes in endocannabinoid levels in the gastrointestinal system after OOS-TMP administration, the exact mechanisms for this remain unknown: it simply represents the fasting conditions in the gastrointestinal system and the effect of OOS-TMP on endocannabinoid metabolizing enzymes left unclear. Further studies are necessary.

Acknowledgements

This work was supported by grants from the Japan International Science and Technology Exchange Center and from the Ministry of Education, Science, Sports and Culture of Japan (for Young Scientists B: 18790378).

References

Aldridge WN, Miles JW, Mount DL, Verschoyle RD. The toxicological properties of impurities in malathion. Arch Toxicol 1979;42:95-100.
Aldridge WN, Dinsdale ED, Nemery B, Verschyole RD. Some aspects of the toxicity of trimethyl and triethyl phosphorothioates. Fundam Appl Toxicol 1985;5:s47–60.
Asakawa A, Inui A, Kaga T, Yuzuriha H, Nagata T, Fujimiya M, et al. A role of ghrelin in neuroendocrine and behavioral responses to stress in mice. Neuroendocrinology 2001;74:143–7.
Cota D, Marsicano G, Tschöp M, Grübler Y, Flachskamm C, Schubert M, et al. The endogenous cannabinoid system affects energy balance via central orexigenic drive and peripheral lipogenesis. J Clin Invest 2003;112:423–31.
Darmani NA. The potent emetogenic effects of the endocannabinoid, 2-AG (2-arachidonoylglycerol) are blocked by Δ9-tetrahydrocannabinol and other cannabinoids. J Pharmacol Exp Ther 2002;1:34–42.
Engeli S, Böhnke J, Feldpausch M, Gorzelniak K, Janke J, Bátkai S, et al. Activation of the peripheral endocannabinoid system in human obesity. Diabetic 2005;54:2838–43.
Felder CC, Nielsen A, Briley EM, Palkovits M, Priller J, Axelrod J, et al. Isolation and measurement of the endogenous cannabinoid receptor agonist, anandamide, in brain and peripheral tissues of human and rat. FEBS Lett 1996;393:231–5.
Gandy J, Imamura T. Cellular responses to O,O,S-trimethyl phosphorothioate-induced pulmonary injury in rats. Toxicol Appl Pharmacol 1985;80:51–7.
Giuffrida A, Piomelli D. Isotope dilution GC/MS determination of anandamide and other fatty acylethanolamides in rat blood plasma. FEBS Lett 1998;422:373–6.
Hansen HS, Moesgaard B, Petersen G, Hansen HH. Putative neuroprotective actions of *N*-acyl-ethanolamines. Pharmacol Ther 2002;95:119–26.
Hasegawa J, Koizumi A. Structure and pulmonary toxicity relationship on O,O-dimethyl *S*-alkyl phosphorothioate esters. Pharmacol Toxicol 1990;66:367–72.
Howlett AC, Barth F, Bonner TI, Cabral G, Casellas P, Devane WA, et al. International Union of Pharmacology classification of cannabinoid receptors. Pharmacol Rev 2002;54:161–202.
Huang LF, Toyoshima M, Asakawa A, Inoue K, Harada K, Kinoshita T, et al. Roles of neuropeptides in O,O,S-trimethylphosphorothioate (OOS-TMP)-induced anorexia in mice. Biochem Biophys Res Commun 2007;362:177–82.
Hummel KP, Dickie MM, Coleman DL. Diabetes, a new mutation in the mouse. Science 1966;153:1127–8.
Imamura T, Gandy J, Fukuto TR. Selective inhibition of rat pulmonary monooxygenase by O, O,S-trimethyl phosphorothioate treatment. Biochem Pharmacol 1983a;32:3191–5.
Imamura T, Hasegawa L, Gandy J, Fukuto TR. Effect of drug metabolism inducer and inhibitor on O,O,S-trimethyl phosphorothioate induced delayed toxicity in rats. Chem-Biol Interact 1983b;45:53–64.
Kirkham TC, Williams CM, Fezza F, Marzo VD. Endocannabinoid levels in rat limbic forebrain and hypothalamus in relation to fasting,feeding and satiation:stimulation of eating by 2-arachidonoylglycerol. Br J Pharmacol 2002;136:550–7.
Koizumi A, Montalbo M, Nguyen Q, Hasegawa L, Imamura T. Neonatal death and lung injury in rats caused by intrauterine exposure to O,O,S-trimethylphosphorothioate. Arch Toxicol 1988;61:378–86.
Mechoulam R, Ben-Shabat S, Hanus L, Ligumsky M, Kaminski NE, Schatz AR, et al. Identification of an endogenous 2-monoglyceride,present in canine gut, that binds to cannabinoid receptors. Biochem Pharmacol 1995;50:83–90.
Ohtaka K, Hamade N, Yamazaki Y, Suzuki M, Koizumi A. A direct involvement of the central nervous system in hypophagia and inhibition of respiratory rate in rats after treatment with O,O,S-trimethyl phosphorothioate. Arch Toxicol 1995;69:559–64.
Onaivi ES, Leonard CM, Ishiguro H, Zhang PW, Lin ZC, Akinshola BE, Uhl GR. Endocannabinoids and cannabinoid receptor genetics. Prog Neurobiol 2002;66:307–44.
Pacher P, Batkai S, Kunos G. The endocannabinoid system as an emerging target of pharmacotherapy. Pharmacol Rev 2006;58:389–462.
Pagotto U, Pasquali R. Fighting obesity and associated risk factors by antagonising cannabinoid type 1 receptors. The Lancet 2005;365:1363–4.
Schmid HHO, Schmid PC, Natarajan V. *N*-acylated glycerophospholipids and their derivatives. Prog Lipid Res 1990;29:1-43.
Schmid PC, Krebsbach RJ, Perry SR, Dettmer TM, Maasson JL, Schmid HH. Occurrence and postmortem generation of anandamide and other long-chain *N*-acylethanolamines in mammalian brain. FEBS Lett 1995;375(1–2):117–20.
Schmid HHO, Schmid PC, Berdyshev EV. Cell signaling by endocannabinoids and their congeners: questions of selectivity and other challenges. Chem Phys Lipids 2002;121:111–34.
Schwartz MW, Woods SC, Porte DJ, Seeley RJ, Baskin DG. Central nervous system control of food intake. Nature 2000;404:661–71.
Shao J, Yamashita H, Qiao L, Friedman JE. Decreased Akt kinase activity and insulin resistance in C57BL/KsJ-Leprdb/db mice. J Endocrinol 2000;167:107–15.
Sugiura T, Kondo S, Sukagawa A, Nakane S, Shinoda A, Itoh K, et al. 2-Arachidonoylglycerol:apossible endogenous cannabinoid receptor ligand in brain. Biochem Biophys Res Commun 1995;215:89–97.
Terrazzino S, Berto F, Dalle Carbonare M, Fabris M, Guiotto A, Bernardini D, et al. Stearoylethanolamide exerts anorexic effects in mice via down-regulation of liver stearoyl-coenzyme A desaturase-1 mRNA expression. FASEB 2004;18:1580–2.
Toyoshima M, Asakawa A, Fujimiya M, Inoue K, Inoue S, Kinboshi M, et al. Dimorphic gene expression patterns of anorexigenic and orexigenic peptides in hypothalamus account male and female hyperphagia in Akita type 1 diabetic mice. Biochem Biophys Res Commun 2007;19:703–8.
Umetsu N, Grose FH, Allahyari R, Abu-El-Haj S, Fukuto TR. Effect of impurities on the mammalian toxicity of technical malathion and acephate. J Agric Food Chem 1977;25:946–53.
Verschoyle RD, Cabral JRP. Investigation of the acute toxicity of some trimethyl and triethyl phosphorothioates with particular reference to those causing lung damage. Arch Toxicol 1982;51:221–31.
Wang J, Takeuchi T, Tanaka S, Kubo SK, Kayo T, Lu D, et al. A mutation in the insulin 2 gene induces diabetes with severe pancreatic beta-cell dysfunction in the Mody mouse. J Clin Invest 1999;103:27–37.
Yang HYT, Karoum F. GC/MS analysis of anandamide and quantification of *N*-arachidonoylphosphatidyl ethanolamides in various brain regions, spinal cord, testis, and spleen of the rat. J Neurochem 1999;72(5):1959–68.
Yoshioka M, Kayo T, Ikeda T, Koizumi A. A novel locus, Mody4, distal to D7Mit189 on chromosome 7 determines early-onset NIDDM in nonobese C57BL/6 (Akita) mutant mice. Diabetes 1997;46:887–94.

European Journal of Immunology

Aberrant splicing of the milk fat globule-EGF factor 8 (MFG-E8) gene in human systemic lupus erythematosus

Hiroshi Yamaguchi[1,2], Takashi Fujimoto[3], Shinobu Nakamura[3], Koichiro Ohmura[4], Tsuneyo Mimori[4], Fumihiko Matsuda[5] and Shigekazu Nagata[1,2,6]

[1] Department of Medical Chemistry, Graduate School of Medicine, Kyoto University, Sakyo, Kyoto, Japan
[2] Department of Integrated Biology, Graduate School of Frontier Bioscience, Osaka University, Osaka, Japan
[3] Department of General Medicine, Nara Medical University, Kashihara, Nara, Japan
[4] Department of Rheumatology and Clinical Immunology, Graduate School of Medicine, Kyoto University, Sakyo, Kyoto, Japan
[5] Center for Genomic Medicine/Inserm U.852, Graduate School of Medicine, Kyoto University, Sakyo, Kyoto, Japan
[6] Core Research for Evolutional Science and Technology, Japan Science and Technology Corporation, Sakyo, Kyoto, Japan

Milk fat globule-EGF factor 8 (MFG-E8) promotes the phagocytosis of apoptotic cells by serving as a bridging molecule between apoptotic cells and phagocytes. Many apoptotic cells are left unengulfed in the germinal centers of the spleen of MFG-E8$^{-/-}$ mice, which develop a human systemic lupus erythematosus (SLE)-like autoimmune disease. Here, we analyzed the MFG-E8 gene in human SLE patients, and found in two out of 322 female patients a heterozygous intronic mutation, which caused a cryptic exon from intron 6 to be included in the transcript. The cryptic exon contained a premature termination codon, generating a C-terminally truncated MFG-E8 protein. The mutant MFG-E8 was aberrantly glycosylated and sialylated, but bound to phosphatidylserine and enhanced the phagocytosis of apoptotic cells. When intravenously injected into mice, the mutant MFG-E8 was sustained longer in the blood circulation than wild-type MFG-E8. Repeated administrations of the mutant MFG-E8 protein induced the production of autoantibodies, such as anti-cardiolipin and anti-nuclear antibodies, at a lower dose than that required for the wild-type protein. These results suggested that the intronic mutation in the human MFG-E8 gene can lead to the development of SLE.

Key words: Aberrant splicing · Apoptosis · Autoimmiune disease · Protein stability

Introduction

Unnecessary or harmful cells are eliminated by apoptosis, a form of programmed cell death in which cysteine proteases of the caspase family are activated to cleave cellular substrates [1, 2]. The apoptotic cells are rapidly engulfed and digested by phagocytes such as macrophages and immature dendritic cells. The swift engulfment of cell corpses by phagocytes prevents the release of noxious or immunogenic debris from dying cells into the circulation. In the process of apoptosis, the dying cells expose phosphatidylserine on their external membrane in a caspase-dependent manner. This externalization of phosphatidylserine is

Correspondence: Professor Shigekazu Nagata
e-mail: snagata@mfour.med.kyoto-u.ac.jp

one of the hallmarks of apoptosis and acts as an "eat me" signal for phagocytes [3]. Recently, several molecules that recognize phosphatidylserine have been identified [4–7].

Systemic lupus erythematosus (SLE) is a chronic autoimmune disease caused by multiple genetic and environmental factors [8]. Patients with SLE develop a broad spectrum of clinical manifestations affecting the skin, kidney, lungs, blood vessels, and/or nervous system. SLE is also characterized by the presence in sera of autoantibodies against nuclear components (anti-RNP and anti-DNA antibodies). Unengulfed apoptotic cells can be found in the germinal centers of the lymph nodes of some SLE patients, and macrophages from these patients show a reduced ability to engulf apoptotic cells [9]. Furthermore, circulating DNA or nucleosomes can also be found in the sera of SLE patients [10, 11]. These results suggest that a deficiency in the clearance of apoptotic cells is one of the causes of SLE.

Milk fat globule-EGF factor 8 (MFG-E8) is a glycoprotein. At the *N*-terminus, it has a EGF-like repeat(s), and at the *C*-terminus, there are two discoidin domains that bind phosphatidylserine. It was originally identified as a component of milk fat globules that bud from the mammary epithelia during lactation. But it is now known to play important roles in various systems such as involution of mammary glands, adhesion between sperm and egg, repair of intestinal mucosa, and angiogenesis [12]. MFG-E8 is secreted by activated macrophages and immature dendritic cells [13], and it promotes the engulfment of apoptotic cells by working as a bridging molecule between apoptotic cells and phagocytes [7]. In MFG-E8-knockout mice, many apoptotic cells are left unengulfed in the germinal centers of the spleen [14]. The MFG-E8$^{-/-}$ mice produce autoantibodies including anti-cardiolipin and anti-dsDNA antibodies and suffer from an SLE-type autoimmune disease. Human MFG-E8 is maintained at the optimal concentration to support the engulfment of apoptotic cells; in excess, MFG-E8 inhibits phagocytosis and causes autoimmune diseases [15, 16].

In this report, we analyzed the human MFG-E8 gene of SLE patients, and found in two female patients an intronic mutation that caused aberrant splicing of intron 6, resulting in the inclusion of a cryptic exon in the transcript. This cryptic exon contained a premature termination codon, which generated an MFG-E8 mutant truncated at the C2-homologous domain. The truncated MFG-E8 (designated as C2del) was abnormally glycosylated with terminal sialic acids; yet, it bound to phosphatidylserine and enhanced the phagocytosis of apoptotic cells. When injected into mice, C2del showed greater stability than wild-type MFG-E8 and induced the production of autoantibodies, suggesting that this mutation of the MFG-E8 gene can lead to the development of SLE in humans.

Results

Analysis of MFG-E8 mRNA in human SLE patients

The human MFG-E8 gene is located on human chromosome 15q25 and is composed of eight exons (National Center for Biotechnology Information GenBank Accession Number WC_000015). To sequence the coding regions of human MFG-E8 gene in a cohort of Japanese female SLE patients ($n = 110$), cDNA was prepared from RNA isolated from the patients' peripheral blood mononuclear cells. Two sets of PCR primers, which amplified the cDNA corresponding to exons 1–5, and exons 4–8 of the human MFG-E8 gene, were prepared (Fig. 1A). No abnormality was found in the cDNA corresponding to the first set of exons (exons 1–5) in any of the 110 patients, but the RT-PCR of exons 4–8 from one patient yielded a longer-than-normal amplicon in addition to the wild-type one (Fig. 1B). A sequence analysis and BLAST search indicated that the long amplicon contained a cryptic exon of 102 bp from intron 6 of the MFG-E8 gene (Fig. 1C). This insertion caused a premature termination of the human MFG-E8 coding sequence.

Aberrant splice-in of a cryptic exon caused by an A-to-G mutation in intron 6

Exons are defined by exonic and intronic *cis*-regulatory elements in addition to the core splice-site motifs [17, 18]. A sequence analysis of the human MFG-E8 chromosomal gene of the patient revealed a heterozygous A-to-G point mutation located 43 bp downstream of the cryptic exon, or 937 bp from exon 5 (IVS 6-937) (Fig. 1C and D). To examine the effect of this point mutation on the pre-mRNA splicing of the human MFG-E8 gene, an MFG-E8 minigene carrying intron 6 was constructed (Fig. 2A). That is, a part of exon 6–7 of the human MFG-E8 cDNA, in pEF-BOS vector [19], was replaced by a DNA fragment of the human MFG-E8 chromosomal gene carrying exon 6, intron 6, and exon 7 from the patient (G-allele at IVS 6-937) or a control (A-allele at IVS 6-937) individual (Fig. 2A). The splicing pattern of the MFG-E8 minigene was then assayed by expression in human HEp-2 cells. Semi-quantitative RT-PCR analysis of the RNA showed that the RNA carrying the cryptic exon was reproducibly about ten times more abundant in the cells transfected with the G-allele minigene than the cells transfected with the A-allele minigene (Fig. 2B). These results indicated that the A-to-G mutation in intron 6 (IVS 6-937 A>G) caused the aberrant inclusion of the cryptic exon in the human MFG-E8 transcript.

A screening of the MFG-E8 chromosomal gene by DNA sequencing revealed the same intronic mutation (IVS 6-937 A>G) in additional one patient out of 212 Japanese female SLE patients, while none of 228 healthy female volunteers carried the mutation.

C2del binds to phosphatidylserine and enhances the phagocytosis of apoptotic cells

Human MFG-E8 consists of a signal sequence, an EGF-like domain carrying an RGD motif, and two Factor VIII C1/C2-homologous domains (Fig. 3A). The MFG-E8 transcript that included the cryptic exon encoded an MFG-E8 protein that was truncated at the C2 domain (designated as C2del) (Fig. 3A). Studies on mouse and bovine MFG-E8 show that the C1/C2-

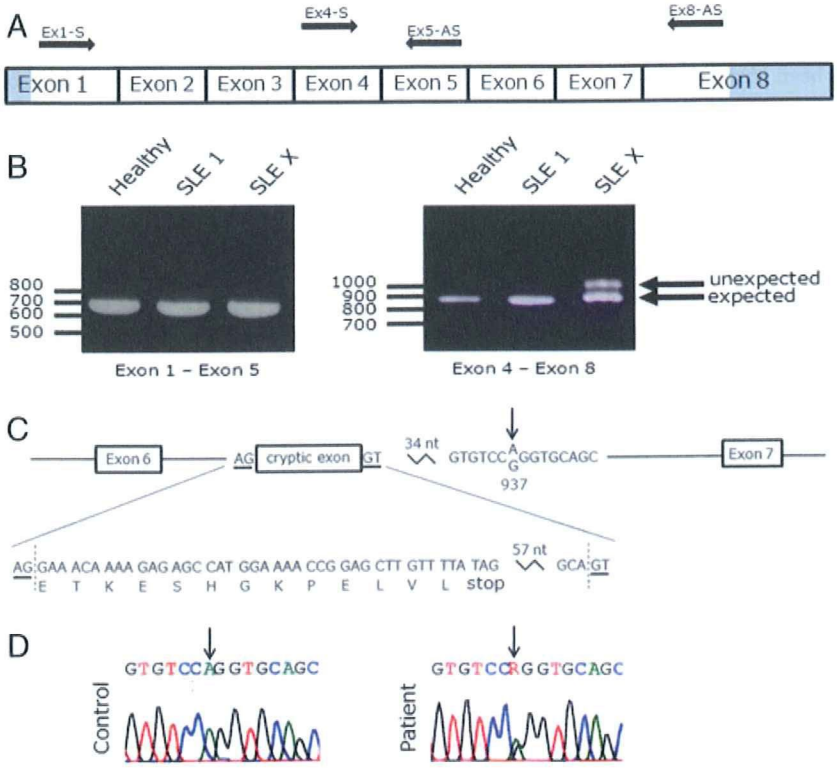

Figure 1. Sequence analysis of the human MFG-E8 gene in SLE patients. (A) Schematic presentation of the human MFG-E8 cDNA and the primers used for PCR. The 5′ and 3′ non-coding regions are indicated as blue boxes. (B) Agarose gel electrophoresis of the RT-PCR product from a healthy person and two SLE patients (SLE 1 and SLE X). PCR were performed with Ex1-S and Ex5-AS (left) or with Ex4-S and Ex8-AS (right). One hundred and ten SLE patients were examined. (C) A cryptic exon in intron 6 of the human MFG-E8 gene. The splice acceptor and donor sites (AG-GT) flanking the cryptic exon are underlined. A partial sequence of the cryptic exon is shown with the deduced amino acid sequence. IVS 6-937 is an A-to-G mutation located 43 bp downstream of the cryptic exon, and indicated by an arrow. (D) The sequence profile of IVS 6-937 and its flanking regions in a control subject (left) and in the patient (right). The position of IVS 6-937 is indicated by an arrow. The SNP in human MFG-E8 gene was submitted to NCBI dbSNP with the submitter SNP (ss) number 184955574.

homologous domains are required for binding to phosphatidylserine [7, 20]. To characterize C2del, we prepared human rMFG-E8 using HeLa cell transformants that produced the transgene in a tetracycline-dependent manner. On SDS-PAGE, the purified C2del ran as a smeared band of approximately 50 kDa, which was significantly bigger than the 46-kDa wild-type MFG-E8 (Fig. 3B). This was unexpected considering that C2del had a truncation of 96 amino acids and contained only one of three *N*-linked glycosylation sites present in the wild-type protein. The treatment of C2del with PNGase F reduced its molecular weight to 32.6 kDa (Fig. 3C), and a mutation of the remaining *N*-glycosylation site (Asn^{238}) also reduced its molecular weight (data not shown). Neuraminidase treatment significantly reduced C2del's molecular weight (Fig. 3D), indicating that it was sialylated. These results suggested that this C-terminal truncation of human MFG-E8 caused it to be aberrantly glycosylated.

We next examined the ability of C2del to recognize apoptotic cells. As shown in Fig. 3E, C2del dose-dependently bound to phosphatidylserine. The dissociation constants (Kd) determined by Biacore for the wild-type and C2del MFG-E8 were 1.1 and 8.0 nM, respectively. C2del supported phagocytosis with a bell-shaped dosage effect and the same dose dependency as the wild-type molecule (Fig. 3F). However, the ability of C2del to enhance the engulfment at the optimum concentration was consistently lower than that observed with the wild-type MFG-E8.

Aberrant *in vivo* stability of C2del and the induction of autoimmune disease

As described above, C2del was aberrantly glycosylated, and in particular, sialylated. The sialylation of proteins is known to prolong their half-life *in vivo* [21, 22]. To examine whether this was true for C2del, the wild-type MFG-E8 and C2del proteins were injected into C57BL/6 mice, and their levels in serum were monitored by ELISA. As shown in Fig. 4A, when 12 pmol of the wild-type or mutant MFG-E8 was injected into the tail vein, about 20 pM wild-type MFG-E8 was found in the serum after 60 min, whereas the concentration of C2del was more than 1 nM at the same time point. These results suggested that C2del was sustained longer than the wild-type protein in the blood.

We previously showed that excess MFG-E8 prevents the efficient engulfment of apoptotic cells and that some SLE patients carry a significantly increased level of MFG-E8 in their blood [15]. Accordingly, the injection of wild-type MFG-E8 into mice induced the development of autoimmune diseases [16]. Since C2del lasted

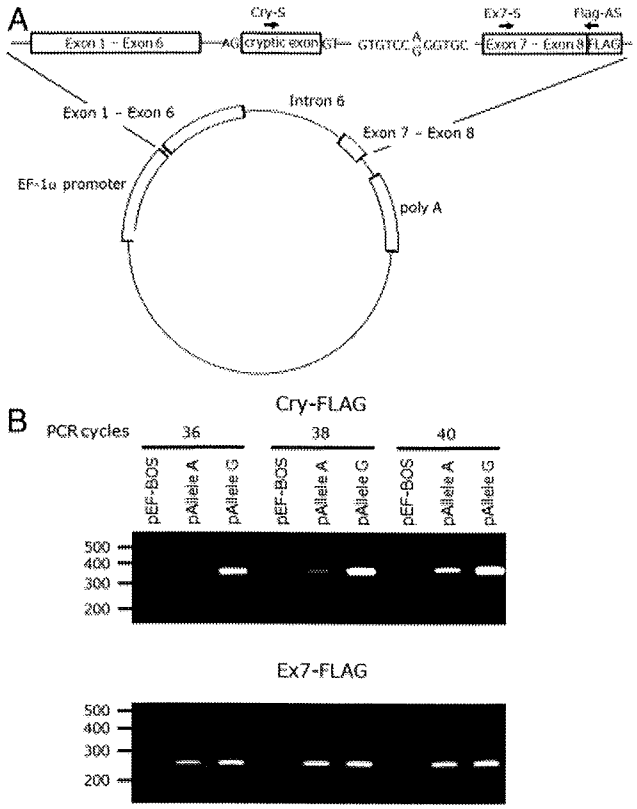

Figure 2. Inclusion of a cryptic exon in the MFG-E8 transcript caused by the IVS 6-937 A>G mutation. (A) Overall structure of the vector used to study the splicing of the MFG-E8 minigene. Human MFG-E8 minigenes, driven by the human EF-1α promoter, were constructed by inserting intron 6 of the A allele (control) and the G allele (patient) into the MFG-E8 cDNA. Positions of the primers (Cry-S, Ex7-S, and Flag-AS) for RT-PCR analysis are indicated by arrows. (B) RT-PCR for the RNA carrying the cryptic exon. The MFG-E8 minigene was transfected with HEp-2 cells, incubated overnight, and treated with 100 μg/mL cycloheximide for 2 h. RT-PCR with the total RNA was performed for the indicated cycles using the primers of Cry-S and Flag-AS (Cry-FLAG) to detect the cryptic exon (upper), or with the primers of Ex7-S and Flag-AS (Ex7-FLAG) to monitor the expression of exon 7 of the MFG-E8 minigene (lower). Transfection into HEp-2 cells and RT-PCR analysis were done independently three times, and representative data are shown.

longer *in vivo* than wild-type MFG-E8, we hypothesized that the administration of C2del might cause autoimmune disease in mice at a lower dose than the wild-type molecule. As shown in Fig. 4B, the repeated injection of C2del induced the production of anti-nuclear antibodies in mice at a dose, with which the wild-type MFG-E8 had little effect. In addition, two out of five mice injected with C2del developed a high level of anti-cardiolipin antibodies (Fig. 4C). These results suggested that C2del could be responsible for the development of SLE in the patient.

Discussion

Approximately 70% of human genes have alternatively spliced transcripts [23]. While alternative splicing generally facilitates the synthesis of a greater variety of proteins, mutations disrupting the splice sites or their regulatory elements can cause hereditary disease through the production of aberrant transcripts [24]. In this report, we described SLE patients whose MFG-E8 mRNA carry an insertion of 102 nt that resembles a cryptic exon. A splicing assay using a human MFG-E8 minigene carrying intron 6 revealed that the aberrant splicing of the MFG-E8 gene was caused by an A-to-G mutation in the intron. The inclusion of the cryptic exon in the transcript, as a result of this mutation, may be explained by the generation of a GGG motif, an intronic splicing enhancer [25, 26], which activates an exon choice by interacting with trans factors that regulate splicing [27, 28]

The cryptic exon incorporated in C2del had a premature termination codon located in the C2 domain of human MFG-E8. In general, mRNA that contain premature termination codons are eliminated by an mRNAs surveillance mechanism called nonsense-mediated mRNA decay (NMD) [29]. In fact, in a splicing assay with the MFG-E8 minigene, the transcripts containing the cryptic exon increased when the premature termination was blocked by treating the cells with cycloheximide or by removing the termination codon with site-directed mutagenesis (data not shown). On the other hand, a significant proportion of the MFG-E8 transcripts from the patient carried the cryptic exon. There are two possible explanations for this discrepancy: (i) the efficiency of NMD is different between HEp-2 and human peripheral blood mononuclear cells [30], and (ii) the mutant transcript may be more stable in the white blood cells of the patient. In addition, the NMD efficiency is known to differ among individuals. For example, the same mutation that leads to premature termination in the dystrophin gene can cause a mild (Becher muscular dystrophy) or more severe (Duchene muscular dystrophy) phenotype in different individuals [31].

Wild-type human MFG-E8 has an apparent M_r of 46 kDa, carries three *N*-glycosylation sites, and is glycosylated. C2del retained only one of the glycosylation sites, yet its molecular weight increased to 50 kDa, due to higher glycosylation. This aberrant glycosylation was observed in other cell lines, such as HEK293T cells (data not shown), confirming that it was an intrinsic property of C2del, and is not due to the host cell lines. The carbohydrate attached to C2del was sialylated, suggesting that the carbohydrate moiety was structurally different from that on the wild-type protein. Missense or truncation mutations in secreted or membrane proteins often cause to abnormal glycosylation and the accumulation of the proteins in the endoplasmic reticulum [32, 33]. We found that when C2del was expressed in HeLa cells, a significant portion of the product remained in the ER, where it was associated with calnexin and GRP78, ER chaperons (data not shown). It is possible that C2del was more heavily glycosylated and sialylated at ER to compensate for its insolubility.

SLE is an autoimmune disease characterized by the presence of autoantibodies, such as anti-nuclear and anti-DNA antibodies [8]. We previously reported that mice injected with MFG-E8 showed symptoms of SLE-like autoimmune disease [16]. Here, we found that C2del induced autoantibody production in mice at a lower dose than wild-type MFG-E8. Since the half-life of C2del in the blood circulation was longer than that of the wild-type protein, it could have interfered more than wild-type with the phosphatidylserine-dependent phagocytosis of apoptotic cells. The same

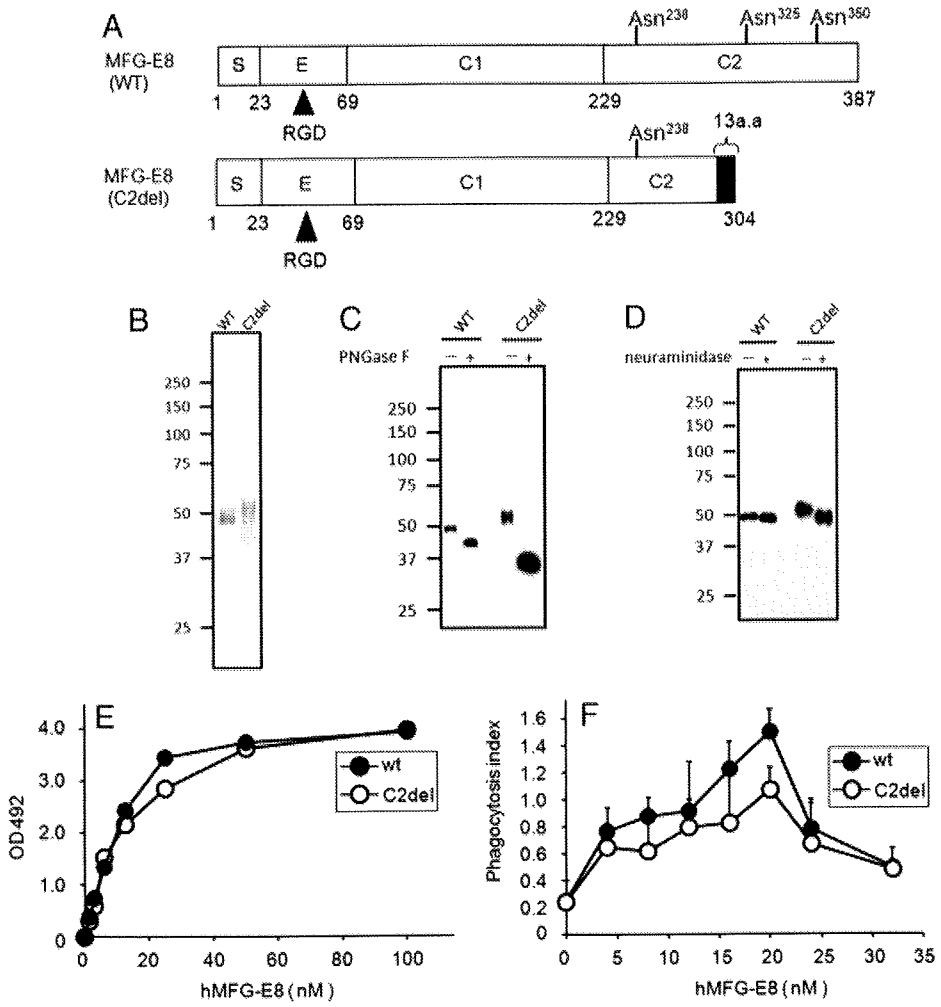

Figure 3. C2del binding to phosphatidylserine, and C2del-dependent phagocytosis of apoptotic cells. (A) Structure of the C2del mutant. C2del was truncated at the C2-homologous domain. Potential N-linked glycosylation sites (Asn^{238}, Asn^{325}, and Asn^{350}) are indicated. An extra 13-amino-acid region at the C-terminus of C2del is indicated as a filled box. S, Signal sequence; E, EGF domain; C1 and C2, Factor VIII-homologous domains; RGD, an Arg-Gly-Asp motif. (B) Preparation of human rMFG-E8. Purified wild-type and C2del MFG-E8 were analyzed by 10% SDS-PAGE and stained with Coomassie brilliant blue. (C) PNGase F treatment. Flag-tagged wild-type or C2del MFG-E8 was subjected to 10% SDS-PAGE before (–) or after (+) PNGase F treatment, and analyzed by Western blotting with an anti-Flag mAb. (D) Neuraminidase treatment. Flag-tagged wild-type or C2del MFG-E8 was subjected to 10% SDS-PAGE before (–) or after (+) neuraminidase digestion, and analyzed by Western blotting with the anti-Flag mAb. (E) Human MFG-E8 binding to phosphatidylserine. The indicated concentrations of wild-type MFG-E8 (•) or C2del (○) were added to a phosphatidylserine-coated microtiter plate. Bound proteins were detected by the anti-Flag mAb. Experiments were done in duplicate, and the mean values are shown. The experiments were done twice, and the representative data are shown. (F) Effect of human MFG-E8 on the phagocytosis of apoptotic cells. Apoptotic thymocytes (2×10^5 cells) were added to NIH3T3 transformants (1×10^4 cells) expressing integrin $\alpha_v\beta_3$ and incubated for 2 h with the indicated concentrations of wild-type MFG-E8 (•) or C2del (○). The cells were TUNEL-stained, and the phagocytosis index is expressed as the number of TUNEL-positive cells *per* phagocyte. The number of TUNEL-positive cells *per* phagocyte were determined for six fields that contain 20–30 phagocytes and is expressed as the phagocytosis index with SD. Data are representative of two independent experiments.

situation may apply in the patient, and the IVS 6-937 A>G mutation in the MFG-E8 gene may be a susceptibility mutation for SLE.

A recent SNP analysis of about 150 SLE patients in Taiwan indicated the predisposition of a specific SNP, causing a replacement of leucine to methionine at the amino acid position of 76 in the MFG-E8 gene, to SLE [34]. Here, we found two out of 322 SLE female patients carry a heterozygous intronic mutation that causes production of aberrant MFG-E8, and detected an aberrantly spliced MFG-E8 mRNA in mononuclear cells of the patient. Since MFG-E8 is mainly produced by Mac-1^+ cells in the immune system, we assume the aberrant MFG-E8 mRNA is produced from monocytes of the patients. In any case, whichever cells produce the aberrant form of the MFG-E8, it can cause SLE-type autoimmune disease. Splicing can be affected not only by *cis*-elements on the chromosomal gene but also by factors that regulate the splicing [35]. The presence of a cryptic exon in the MFG-E8 gene suggests that abnormal deviation in the splicing mechanism for the MFG-E8 gene can lead to the production of aberrant MFG-E8 protein. To elucidate the involvement of MFG-E8 in SLE pathogenesis in more detail, it will be necessary to analyze

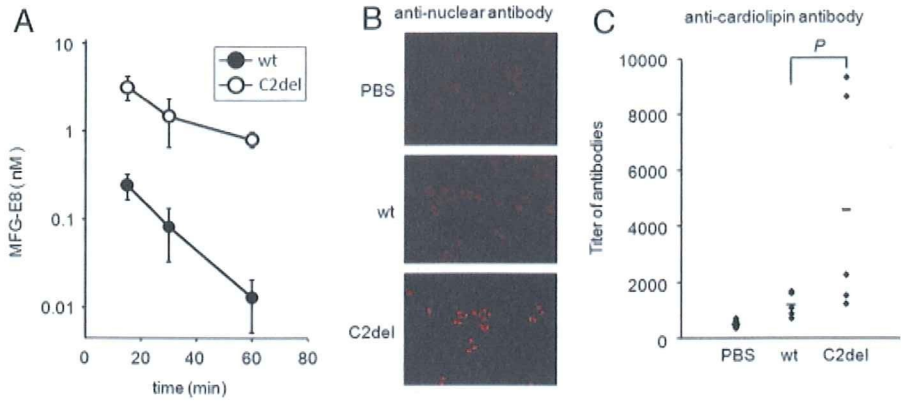

Figure 4. Production of autoantibodies in mice by C2del. (A) Clearance of human MFG-E8 from the blood circulation. Four mice were injected intravenously with 12 pmol of wild-type human MFG-E8 (●) or C2del (○), and bled at the indicated time points. The concentration of human MFG-E8 in serum was measured by an indirect ELISA as described in the *Materials and methods*. The mean concentrations are plotted with SD. (B) Detection of anti-nuclear antibodies by immunofluorescence on HEp-2. Five C57BL/6 female mice were injected intravenously with 12 pmol of wild-type or C2del weekly for four times. Blood samples were obtained 2 wk after the last injection. Human HEp-2 cells were incubated with 50-times diluted serum, and the antibodies bound to the cells were detected by Cy3-cojugated $F(ab')_2$ of goat anti-mouse IgG. All five mice gave a similar result, and representative results are shown. (C) Titer of anti-cardiolipin antibody. Five C57BL/6 female mice were injected intravenously with 12 pmol of wild-type or C2del weekly for six times. Blood samples were obtained 1 wk after the last injection, and the titer for anti-cardiolipin antibody was determined by ELISA as described in the *Materials and methods*. Average values obtained with five mice are indicated by horizontal bars. *p*-value, determined by Mann–Whitney's *U*-test, was 0.095.

comprehensively the MFG-E8 gene and its expression mechanism.

Materials and methods

Subjects

Blood mononuclear cells were collected from 110 female SLE patients at Nara Medical University Hospital, and 212 female SLE patients at Kyoto University Hospital. All the patients gave written informed consent. The ethical committees of the Graduate School of Medicine, Osaka University, the Graduate School of Medicine, Kyoto University, and Nara Medical University Hospital approved our study. Genomic DNA and RNA were prepared from the blood mononuclear cells using Gentra Puregene Blood kit (Qiagen) and Isogen-LS (Nippon Gene), respectively, and cDNA was synthesized with random hexamer as a primer.

Direct sequencing of the human MFG-E8 cDNA and chromosomal gene

The human MFG-E8 cDNA was amplified by PCR using the following two sets of primers: Ex1-S (5′-GTCTGAGCAGCC-CAGCGT-3′) and Ex5-AS (5′-AGAGTGCAGGCCGTGTGGCA-3′); and Ex4-S (5′-GAACCTGCTGCGGAGGATGT-3′) and Ex8-AS (5′-GGCCCATGGAAAGCAGGAAG-3′). The PCR products were purified with a NucleoFast 96 PCR Plate (Macherey-Nagel). Cycle sequencing was performed using a BigDye Terminator v3.1 Cycle Sequencing kit and ABI 3100 genetic analyzer (Applied Biosystems). For sequencing the intron 6 of the MFG-E8 chromosomal gene, a DNA fragment was amplified by PCR using the following primers: (GGGACCTCTCCCTTGAGCAC and CCAGTTCG-CACTGTCATTAC), and subjected to the cycle sequencing.

Splicing assay with a minigene

The normal and mutant (IVS 6-937) alleles of intron 6 in the human MFG-E8 gene were amplified from the genomic DNA of the SLE patient. The 1791 bp PstI-ApaI fragment carrying intron 6 was used to replace part (52 bp of PstI-ApaI DNA fragment) of the human MFG-E8 cDNA in pEF-BOS-hMFG-E8-Flag [15], and the product was verified by DNA sequencing. The minigene was introduced into HEp-2 cells by lipofection using Fugene 6 (Roche). Briefly, 1×10^5 cells were transfected with 0.5 μg DNA and cultured overnight in DMEM containing 10% FCS. After treating the cells for 2 h with 100 μg/mL cycloheximide, the total RNA was extracted from the cells using an RNeasy Mini Kit (Qiagen). The cDNA was synthesized with high capacity RNA-to-cDNA kit (Applied Biosystems) and subjected to PCR with the following primers: Cry-S, 5′-GCAGGACGATGATCTGCCTA-3′; Ex7-S, 5′-CGTAACTTTGGCTCTGTCCA-3′; and Flag-AS 5′-CGTC-CTTGTAGTCGCTAGCA-3′.

Human rMFG-E8, binding to phosphatidylserine, and phagocytosis assay

To prepare human rMFG-E8, the cDNA for the Flag-tagged human MFG-E8 was inserted into pTRE2 expression vector (Clontech), and introduced into HAM3 cells, a HeLa tet-on cell

line [36], with a vector carrying the hygromycin-resistance gene. After selection with 0.5 mg/mL hygromycin, the transformant clones that produced MFG-E8 in a doxycycline-induced manner were selected. To produce MFG-E8, the transformants were treated with 1 μg/mL doxycycline in DMEM containing 1% FCS, and the secreted MFG-E8 was purified using anti-Flag M2 affinity gel (Sigma-Aldrich). To analyze the sugar moiety attached to human MFG-E8, rMFG-E8 (35 ng protein) was incubated at 37°C for 1 h with 0.1 unit of neuraminidase (Nacalai) or 500 units of PNGase F (New England Biolabs) and subjected to 10% SDS-PAGE, followed by Western blotting using an anti-Flag mAb.

The binding of hMFG-E8 to phosphatidylserine was determined by the solid-phase ELISA as described [20]. The Biacore technology using BiacoreX (GE Healthcare) with a HPA sensor chip was utilized to determine the dissociation constant for the binding of hMFG-E8 to phosphatidylserine according to Saenko *et al.* [37].

Phagocytosis was assayed as described previously [7] with NIH3T3 cell transformants expressing $\alpha_v\beta_3$ integrin as phagocytes and apoptotic $CAD^{-/-}$ thymocytes as preys. After engulfment, the cells were stained with TUNEL using an ApopTag peroxidase *in situ* apoptosis detection kit (Chemicon). The phagocytosis index was determined as the number of TUNEL-positive cells *per* phagocyte.

Injection of recombinant proteins

All animal experiments were carried out in accordance with protocols approved by the Animal Care and Use Committee of the Kyoto University Graduate School of Medicine. Human rMFG-E8 (12 pmol in 300 μL of PBS containing 2.5% serum from C57BL/6 mice) was intravenously administered into 8-wk-old C57BL/6 female mice through the tail vein. Serum was harvested 15, 30, and 60 min after the injection, and the MFG-E8 level was measured by an indirect sandwich ELISA. In brief, a 96-well Maxisorp plate (Nalge Nunc International) was coated with 1 μg/well of anti-FLAG mAb in 50 mM sodium bicarbonate buffer (pH 9.6) and incubated with Reagent Diluent Concentrate 2 (R&D Systems). Triton X-100 was added to the serum samples at a final concentration of 1%, the samples were diluted ten times with TBS, and a 50-μL aliquot was applied to each well. After a 1-h incubation, the wells were washed with wash buffer supplied with the Ampli Q kit (Dako), incubated with 0.8 μg/mL biotinylated hamster mAb against human MFG-E8 (clone 2–8E4A)[15], washed as above, and incubated with 8000-times-diluted alkaline phosphatase-conjugated streptavidin (Dako) for 30 min. The alkaline phosphatase activity was measured using the Ampli Q kit. Human rMFG-E8 diluted with 10% normal mouse serum was used to prepare the standard curve.

Detection of autoantibodies

C57BL/6 female mice at the age of 10 wk were treated weekly with 12 pmol of hMFG-E8 for a total of four or six times, and sera were collected before, and 6 and 7 wk after the first injection. The concentration of anti-cardiolipin antibody in the sera was measured by ELISA. In brief, 1 μg of cardiolipin in 100 μL of methanol was added to a 96-well plate (Immulon 1B microtiter plate; Thermo Labsystems), and the plate was air-dried. After blocking with 10% FCS, serially diluted mouse serum was added to the wells. After a 1-h incubation at room temperature, the mouse antibodies bound to the plate were detected using HRP-conjugated goat anti-mouse Ig (Dako) and peroxidase-detecting kit (Sumitomo Bakelite). The color reaction was read at 492 nm using a microplate reader (Titertek Instruments), and the titer of the antibody was defined as the dilution that gave the absorbance of 0.1.

Anti-nuclear antibody was detected by indirect immunofluorescence. In brief, human HEp-2 cells cultured on a glass slide were fixed with cold acetone and incubated with 50-times-diluted mouse serum at 37°C for 30 min. The antibodies bound to the HEp-2 cells were detected by Cy3-conjugated $F(ab')_2$ of goat anti-mouse IgG (Jackson ImmunoResearch Laboratories) diluted 100 times with PBS/10% normal goat serum, and observed by fluorescence microscopy (Biorevo, Keyence).

Acknowledgements: The authors thank M. Fujii and M. Harayama for secretarial assistance. This work was supported in part by Grants-in-Aid for Specially Promoted Research from the Ministry of Education, Science, Sports, and Culture in Japan to S. N. H. Y. was a Research Assistant for Osaka University Global COE program (System Dynamics of Biological Function).

Conflict of interest: The authors declare no financial or commercial conflict of interest.

References

1 **Adams, J. M.,** Ways of dying: multiple pathways to apoptosis. *Genes Dev.* 2003. 17: 2481–2495.

2 **Fischer, U., Janicke, R. U. and Schulze-Osthoff, K.,** Many cuts to ruin: a comprehensive update of caspase substrates. *Cell Death Differ.* 2003. 10: 76–100.

3 **Fadok, V. A., Bratton, D. L., Frasch, S. C., Warner, M. L. and Henson, P. M.,** The role of phosphatidylserine in recognition of apoptotic cells by phagocytes. *Cell Death Differ.* 1998. 5: 551–562.

4 **Park, D., Tosello-Trampont, A. C., Elliott, M. R., Lu, M., Haney, L. B., Ma, Z., Klibanov, A. L. *et al.*,** BAI1 is an engulfment receptor for apoptotic cells upstream of the ELMO/Dock180/Rac module. *Nature* 2007. 450: 430–434.

5 **Park, S. Y., Jung, M. Y., Kim, H. J., Lee, S. J., Kim, S. Y., Lee, B. H., Kwon, T. H. *et al.*,** Rapid cell corpse clearance by stabilin-2, a membrane phosphatidylserine receptor. *Cell Death Differ.* 2008. 15: 192–201.

6 **Miyanishi, M., Tada, K., Koike, M., Uchiyama, Y., Kitamura, T. and Nagata, S.,** Identification of Tim4 as a phosphatidylserine receptor. *Nature* 2007. 450: 435–439.

7 **Hanayama, R., Tanaka, M., Miwa, K., Shinohara, A., Iwamatsu, A. and Nagata, S.,** Identification of a factor that links apoptotic cells to phagocytes. *Nature* 2002. 417: 182–187.

8 D'Cruz, D. P., Khamashta, M. A. and Hughes, G. R., Systemic lupus erythematosus. *Lancet* 2007. **369**: 587–596.

9 Gaipl, U. S., Voll, R. E., Sheriff, A., Franz, S., Kalden, J. R. and Herrmann, M., Impaired clearance of dying cells in systemic lupus erythematosus. *Autoimmun. Rev.* 2005. **4**: 189–194.

10 Steinman, C. R., Circulating DNA in systemic lupus erythematosus. Isolation and characterization. *J. Clin. Invest.* 1984. **73**: 832–841.

11 Rumore, P. M. and Steinman, C. R., Endogenous circulating DNA in systemic lupus erythematosus. Occurrence as multimeric complexes bound to histone. *J. Clin. Invest.* 1990. **86**: 69–74.

12 Raymond, A., Ensslin, M. A. and Shur, B. D., SED1/MFG-E8: a bi-motif protein that orchestrates diverse cellular interactions. *J. Cell Biochem.* 2009. **106**: 957–966.

13 Miyasaka, K., Hanayama, R., Tanaka, M. and Nagata, S., Expression of milk fat globule epidermal growth factor 8 in immature dendritic cells for engulfment of apoptotic cells. *Eur. J. Immunol.* 2004. **34**: 1414–1422.

14 Hanayama, R., Tanaka, M., Miyasaka, K., Aozasa, K., Koike, M., Uchiyama, Y. and Nagata, S., Autoimmune disease and impaired uptake of apoptotic cells in MFG-E8-deficient mice. *Science* 2004. **304**: 1147–1150.

15 Yamaguchi, H., Takagi, J., Miyamae, T., Yokota, S., Fujimoto, T., Nakamura, S., Ohshima,S. *et al.*, Milk fat globule EGF factor 8 in the serum of human patients of systemic lupus erythematosus. *J. Leukoc. Biol.* 2008. **83**: 1300–1307.

16 Asano, K., Miwa, M., Miwa, K., Hanayama, R., Nagase, H., Nagata, S. and Tanaka, M., Masking of phosphatidylserine inhibits apoptotic cell engulfment and induces autoantibody production in mice. *J. Exp. Med.* 2004. **200**: 459–467.

17 Wang, Z. and Burge, C. B., Splicing regulation: from a parts list of regulatory elements to an integrated splicing code. *RNA* 2008. **14**: 802–813.

18 Hertel, K. J., Combinatorial control of exon recognition. *J. Biol. Chem.* 2008. **283**: 1211–1215.

19 Mizushima, S. and Nagata, S., pEF-BOS, a powerful mammalian expression vector. *Nucleic Acids Res.* 1990. **18**: 5322.

20 Andersen, M. H., Berglund, L., Rasmussen, J. T. and Petersen, T. E., Bovine PAS-6/7 binds $\alpha_v\beta_5$ integrins and anionic phospholipids through two domains. *Biochemistry* 1997. **36**: 5441–5446.

21 Gregoriadis, G., Jain, S., Papaioannou, I., Laing, P., Improving the therapeutic efficacy of peptides and proteins: a role for polysialic acids. *Int. J. Pharm.* 2005. **300**: 125–130.

22 Chitlaru, T., Kronman, C., Zeevi,M., Kam, M., Harel, A., Ordentlich, A., Velan, B. and Shafferman, A., Modulation of circulatory residence of recombinant acetylcholinesterase through biochemical or genetic manipulation of sialylation levels. *Biochem. J.* 1998. **336**: 647–658.

23 Johnson, J. M., Castle, J., Garrett-Engele, P., Kan, Z., Loerch, P. M., Armour, C. D., Santos,R. *et al.*, Genome-wide survey of human alternative pre-mRNA splicing with exon junction microarrays. *Science* 2003. **302**: 2141–2144.

24 Wang, G. S. and Cooper, T. A., Splicing in disease: disruption of the splicing code and the decoding machinery. *Nat. Rev. Genet.* 2007. **8**: 749–761.

25 McCullough, A. J. and Berget, S. M., G triplets located throughout a class of small vertebrate introns enforce intron borders and regulate splice site selection. *Mol. Cell. Biol.* 1997. **17**: 4562–4571.

26 Yeo, G., Hoon, S., Venkatesh, B. and Burge, C. B., Variation in sequence and organization of splicing regulatory elements in vertebrate genes. *Proc. Natl. Acad. Sci. USA* 2004. **101**: 15700–15705.

27 Chou, M. Y., Rooke, N., Turck, C. W. and Black, D. L., hnRNP H is a component of a splicing enhancer complex that activates a c-src alternative exon in neuronal cells. *Mol. Cell. Biol.* 1999. **19**: 69–77.

28 McCullough, A. J. and Berget, S. M., An intronic splicing enhancer binds U1 snRNPs to enhance splicing and select 5′ splice sites. *Mol. Cell. Biol.* 2000. **20**: 9225–9235.

29 Wen, J. and Brogna, S., Nonsense-mediated mRNA decay. *Biochem. Soc. Trans.* 2008. **36**: 514–516.

30 Bateman, J. F., Freddi, S., Nattrass, G. and Savarirayan, R., Tissue-specific RNA surveillance? Nonsense-mediated mRNA decay causes collagen X haploinsufficiency in Schmid metaphyseal chondrodysplasia cartilage. *Hum. Mol. Genet.* 2003. **12**: 217–225.

31 Kerr, T. P., Sewry, C. A., Robb, S. A. and Roberts, R. G., Long mutant dystrophins and variable phenotypes: evasion of nonsense-mediated decay? *Hum. Genet.* 2001. **109**: 402–407.

32 Morrissette, J. D., Colliton, R. P. and Spinner, N. B., Defective intracellular transport and processing of JAG1 missense mutations in Alagille syndrome. *Hum. Mol. Genet.* 2001. **10**: 405–413.

33 Cheng, S. H., Gregory, R. J., Marshall, J., Paul, S., Souza, D. W., White, G. A., O'Riordan, C. R. and Smith, A. E., Defective intracellular transport and processing of CFTR is the molecular basis of most cystic fibrosis. *Cell* 1990. **63**: 827–834.

34 Hu, C., Wu, C., Tsai, H., Chang, S., Tsai, W. and Hsu, P., Genetic polymorphism in milk fat globule-EGF factor 8 (MFG-E8) is associated with systemic lupus erythematosus in human. *Lupus* 2009. **18**: 676–681.

35 Chen, M. and Manley, J. L., Mechanisms of alternative splicing regulation: insights from molecular and genomics approaches. *Nat. Rev. Mol. Cell Biol.* 2009. **10**: 741–754.

36 Watanabe-Fukunaga, R., Iida, S., Shimizu, Y., Nagata, S. and Fukunaga, R., SEI family of nuclear factors regulates p53-dependent transcriptional activation. *Genes Cells* 2005. **10**: 851–860.

37 Saenko, E., Sarafanov, A., Ananyeva, N., Behre, E., Shima, M., Schwinn, H. and Josic, D., Comparison of the properties of phospholipid surfaces formed on HPA and L1 biosensor chips for the binding of the coagulation factor VIII. *J. Chromatogr. A* 2001. **921**: 49–56.

38 Kawane, K., Fukuyama, H., Yoshida, H., Nagase,H., Ohsawa, Y., Uchiyama, Y., Iida, T. *et al.*, Impaired thymic development in mouse embryos deficient in apoptotic DNA degradation. *Nat. Immunol.* 2003. **4**: 138–144.

Abbreviations: **MFG-E8:** milk fat globule-EGF factor 8 · **NMD:** nonsense-mediated mRNA decay · **SLE:** systemic lupus erythematosus

Full correspondence: Professor Shigekazu Nagata, Department of Medical Chemistry, Graduate School of Medicine, Kyoto University, Yoshida-Konoe, Sakyo, Kyoto 606-8501, Japan
Fax: +81-75-753-9446
e-mail: snagata@mfour.med.kyoto-u.ac.jp

Current address: Shinobu Nakamura, Medical Corporation Katsurakai Hirao Hospital, 6-28 Hyobu, Kashihara, Nara 634-0076, Japan

Received: 27/10/2009
Revised: 5/2/2010
Accepted: 25/2/2010
Accepted article online: 8/3/2010

Eye (2009), 1–7

www.nature.com/eye

LABORATORY STUDY

ARMS2/HTRA1 and *CFH* polymorphisms are not associated with choroidal neovascularization in highly myopic eyes of the elderly Japanese population

H Nakanishi[1,2], N Gotoh[1,2], R Yamada[2,3], K Yamashiro[1], A Otani[1], H Hayashi[1,2], A Tsujikawa[1], N Shimada[4], K Ohno-Matsui[4], M Mochizuki[4], M Saito[5], K Saito[5], T Iida[5], F Matsuda[2,6] and N Yoshimura[1]

Abstract

Purpose **The purpose of this study was to investigate whether the genetic risk factors of age-related macular degeneration (AMD) are associated with the development of choroidal neovascularization (CNV) in highly myopic eyes of elderly Japanese.**

Methods **Highly myopic elderly Japanese patients with and without CNV were genotyped for three AMD-associated single nucleotide polymorphisms (SNPs), namely rs10490924 (A69S) of *ARMS2*, rs11200638 of *HTRA1*, and rs1061170 (Y402H) of complement factor H (*CFH*), with the TaqMan SNP assay. One hundred and eighty-three unrelated highly myopic (axial lengths >26.00 mm or refractive errors >-6.0 diopters) Japanese patients with CNV who were $\geqslant 50$ years of age (mean age $\pm$ standard deviation of 62.7 ± 6.3 years) and 170 highly myopic patients without CNV who were $\geqslant 50$ years old (62.3 ± 7.1 years) were studied. The differences in the genotypic distributions for the three SNPs between the two groups were tested with the Trend χ^2 test, and logistic regression analyses were performed for age and gender adjustment.**

Results **No significant difference was detected in the distribution of the three SNPs, rs10490924 ($P>0.1$), rs11200638 ($P>0.1$), and rs1061170 ($P>0.5$), between the two groups even after adjustments for age and gender differences.**

Conclusion **The genetic risk factors of AMD related to these SNPs do not contribute significantly to the development of CNV in a highly myopic elderly Japanese population.**

Eye advance online publication, 14 August 2009; doi:10.1038/eye.2009.215

Keywords: age-related macular degeneration; myopia; choroidal neovascularization; single nucleotide polymorphism; case–control association study; clinical genetics

Introduction

Choroidal neovascularization (CNV) is one of the most vision-threatening complications in highly myopic eyes. The pathogenesis of CNV in high myopia has not been fully determined. One important causative factor of CNV in highly myopic eyes is related to the excessive axial elongation of the eye, which results in the rupture of the Bruch membrane and atrophy of the choirocapillaries.[1] Patchy chorioretinal atrophy and lacquer cracks are important predisposing findings for the development of CNV in highly myopic eyes.[2] However, there are many highly myopic patients with these ocular predisposing findings who never develop CNV throughout life. This suggests that factors other than excessive axial elongation may also contribute to the development of CNV in these highly myopic eyes.

CNV is a complication common to high myopia and age-related macular degeneration (AMD).[3] High myopia is the most common cause of CNV in patients younger than 50 years of age, whereas CNV can also develop in highly myopic eyes of the elderly population.[4] In the elderly population, the most frequent cause of CNV is AMD; this raises a hypothesis that the

[1]Department of Ophthalmology and Visual Sciences, Kyoto University Graduate School of Medicine, Kyoto, Japan

[2]Center for Genomic Medicine, Kyoto University Graduate School of Medicine, Kyoto, Japan

[3]Human Genome Center, Institute of Medical Science, University of Tokyo, Tokyo, Japan

[4]Department of Ophthalmology and Visual Science, Tokyo Medical and Dental University Graduate School, Tokyo, Japan

[5]Department of Ophthalmology, Fukushima Medical University, Fukushima, Japan

[6]Centre National de Génotypage, Evry Cedex, France

Correspondence: H Nakanishi, Department of Ophthalmology and Visual Sciences, Kyoto University Graduate School of Medicine, Shogoinkawaharacho 54, Sakyo-ku, Kyoto 606 8507, Japan
Tel: +81 75 751 3248; Fax: +81 75 752 0933.
E-mail: hideon@kuhp.kyoto-u.ac.jp

Received: 11 February 2009
Accepted in revised form: 16 July 2009

processes involved in the aetiology of AMD may contribute to the development of CNV in highly myopic patients over the age of 50. AMD is caused by interactions of environmental and genetic factors, and it is believed that genetic factors contribute strongly to AMD.[5–7] Thus, AMD-associated genetic factors may also be associated with the development of CNV in highly myopic eyes of elderly patients.

Among the genetic factors of AMD investigated, a single nucleotide polymorphism (SNP) rs1061170, which is also known as Y402H, of the complement factor H (*CFH*) gene on chromosome 1q32 has been shown in many studies to be a major AMD-associated polymorphism.[8–19] More recently, two SNPs in the *ARMS2(LOC387715)/HTRA1* region on chromosome 10q26, that is rs10490924 (also known as A69S) and rs11200638, were found in many studies to be strongly associated with AMD.[14,19–33] Fernandez-Robredo *et al* hypothesized that CNV associated with AMD and CNV associated with high myopia share a common genetic origin.[34] This group analysed a possible association between two AMD-associated SNPs (rs1061170 and rs10490924) and CNV associated with high myopia in a Spanish population, and they did not find a significant association. However, the possible association in Asian populations remains to be elucidated.

To investigate the possible contribution of AMD genetic risk factors to CNV in elderly highly myopic Japanese, we analysed the association of these AMD-associated SNPs, namely rs10490924 (A69S) of *ARMS2/LOC387715*, rs11200638 of *HTRA1*, and rs1061170 (Y402H) of *CFH*, with the development of CNV in elderly Japanese patients with high myopia.

Materials and methods

All procedures used in this study conform to the tenets of the Declaration of Helsinki. The Institutional Review Board and the Ethics Committee of each institution approved the protocols used in this study. All of the patients were fully informed of the purpose and procedures, and a written consent was obtained from each patient.

Patients and controls

One hundred and eighty-three unrelated highly myopic Japanese patients with CNV (HM-CNV group) who were $\geqslant$50 years of age (mean age $\pm$ standard deviation (SD), 62.7 $\pm$ 6.3 years; men:women, 23.5:76.5%) were recruited from Kyoto University Hospital, Tokyo Medical and Dental University Hospital, and Fukushima Medical University Hospital. The inclusion criteria were (1) axial lengths $>$26.00 mm or refractive errors $>-$6.0 diopters (D) in both eyes, (2) clinical presentation and angiographic manifestations of macular CNV in at least one eye, and (3) age $\geqslant$50 years at their first visit with CNV to our institutes. Among the patients, 141 patients (77%) had monocular CNV and 42 patients (23%) had binocular CNV (an old CNV was present in the fellow eye). All of the patients underwent detailed ophthalmologic examinations, including dilated indirect and contact lens slit-lamp biomicroscopy, automatic objective refraction, measurement of the axial length by A-scan ultrasound (UD-6000, Tomey, Nagoya, Japan) or partial coherence interferometry (IOLMaster, Carl Zeiss Meditec, Dublin, CA, USA), colour fundus photography, optical coherence tomography, and fluorescein angiography. Individuals with a history of ocular surgery, with the exception of cataract surgery, were excluded. Patients with secondary choroidal neovascular diseases, such as angioid streaks, presumed ocular histoplasmosis syndrome, and ocular trauma, were also excluded. Even if patients with CNV had soft drusen in each of their eyes, they were not excluded from this study. However, there was only one highly myopic patient with CNV who also had soft drusen.

For control, 170 highly myopic (axial lengths $>$26.00 mm or refractive errors $>-$6.0 D in both eyes) Japanese cases who were $\geqslant$50 years of age (62.3 $\pm$ 7.1 years; men:women, 31.2:68.8%) without CNV were recruited from the same institutions (HM-control group). Subjects with soft drusen were excluded from the HM-control group.

For a population-based control (PB-control) group, 374 Japanese subjects (39.2 $\pm$ 9.6 years; men:women, 50.8:49.2%) were randomly selected from the Pharma SNP Consortium. This healthy, population-based cohort had been recruited for earlier genomic studies and was considered to be representative of the general Japanese population.[35] None of the subjects in this group had a history of any ocular diseases.

Genotyping

To investigate a possible association between CNV in highly myopic elderly patients and the genetic risk factors of AMD, we genotyped the three AMD-associated SNPs, namely rs10490924 (A69S) of *ARMS2/LOC387715*, rs11200638 of *HTRA1*, and rs1061170 (Y402H) of *CFH*, which have repeatedly been shown to be significantly associated with AMD.

Genomic DNA was prepared from the leucocytes of the peripheral blood using a DNA extraction kit (QuickGene-610L, Fujifilm, Minato, Tokyo, Japan). The public dbSNP database build 128 was used to extract the genotyping information for the SNPs. All of the SNPs were genotyped using Taqman SNP assays with the ABI PRISM 7700 system (Applied Biosystems,

Foster City, CA, USA) according to the manufacturer's instructions.

Statistical analyses

The Hardy–Weinberg equilibrium (HWE) for the genotypic distribution was evaluated using the HWE-exact test for each group. Differences in the demographic features between the HM-CNV group and the HM-control group or the PB-control group were tested for statistical significance by the χ^2 test for dichotomous data and by the Wilcoxon rank sum test for continuous data. Differences in the observed genotypic distribution between the HM-CNV group and the HM-control group were tested by the Trend χ^2 test. Logistic regression analysis was performed for age and gender adjustments. These statistical analyses were performed using software R (http://www.r-project.org/).

The D′ for pairwise linkage disequilibrium (LD) index between rs10490924 and rs11200638, both on chromosome 10q26, was calculated. Differences in the inferred haplotype frequencies between the HM-CNV group and the HM-control group were also examined by the χ^2 test, and multiple testing correction for the *P*-value (*Pc*) was performed by the permutation test (number of iterations = 10 000).[36] Haplotype analyses were performed using the Haploview version 4.0.[37]

The single SNP analyses and the haplotype analyses between the HM-CNV group and the PB-control group were performed in the same way. The level of statistical significance was set at $P<0.05$ and $Pc<0.05$.

Results

The demographics of the study population are shown in Table 1. The HM-CNV group and the HM-control group were not age or gender matched, and the HM-control group was younger and had a higher male-to-female ratio than the HM-CNV group. However, these differences were not significant ($P>0.1$ for age and $P>0.1$ for gender). Both the HM-CNV group and the HM-control group were significantly older than the population-based control group because highly myopic patients ⩾50 years old were recruited and had lower male-to-female ratios because high myopia is a phenotype seen more frequently in women than in men.

The genotype counts, associations, and odds ratio (OR) for rs10490924, rs11200638, and rs1061170 in the HM-CNV group and the HM-control group are shown in Table 2. The distributions of the genotypes for the three SNPs were all in HWE ($P>0.1$). The differences in the genotypic distributions for the three SNPs between the HM-CNV group and the HM-control group were not statistically significant ($P>0.1$). After correcting for

Table 1 Characteristics of the study population

	High myopia ⩾50 years old			*Population-based control (PB-control group)*
	With CNV (HM-CNV group)	*Without CNV (HM-control group)*	*P-value*	
Number of patients	183	170		374
Age (years)				
Range (median)	50–78 (63)	50–79 (61)	0.26[a]	29–58 (34)
Mean ± SD	62.7 ± 6.3	62.3 ± 7.1		39.2 ± 9.6
Gender, number (%)				
Male	43 (23.5%)	53 (31.2%)	0.11[b]	190 (50.8%)
Female	140 (76.5%)	117 (68.8%)		184 (49.2%)
Axial length (mm)[c]				
Range (median)	26.48–35.44 (28.77)	26.49–35.55 (29.29)	<0.01[a]	NA
Mean ± SD	29.00 ± 1.64	29.38 ± 1.81		NA
Number of phakic eyes	219	223		NA
Refractive power of the phakic Eyes (Diopters, mean ± SD)	−12.83 ± 4.46	−13.18 ± 4.60		NA

CNV, choroidal neovascularization; NA, not available; SD, standard deviation.
[a]Wilcoxon rank sum test.
[b]χ^2 test.
[c]Axial length of the both eyes (366 eyes in HM-CNV group and 340 eyes in HM-control group).

Table 2 Genotype counts, associations, and odds ratios for rs10490924, rs11200638, and rs1061170 in the HM-CNV group and the HM-control group

SNP	*Genotype*[a]	*HM-CNV group* (n = 183)		*HM-control* (n = 170)		*Nominal P*[c]	*Age and gender adjusted*[d]	
		Genotype count	*HWE P*[b]	*Genotype count*	*HWE P*[b]		*P*	*OR (95% CI)*
rs10490924 *ARMS2* Ala69Ser	GG/GT/TT	60/92/27	0.44	73/72/24	0.40	0.15	0.16	1.25 (0.92–1.70)
rs11200638 *HTRA1*(−625G > A)	GG/GA/AA	57/95/28	0.29	67/76/26	0.62	0.27	0.28	1.19 (0.87–1.61)
rs1061170 *CFH* Tyr402His	TT/TC/CC	160/22/0	1.00	146/16/1	0.39	0.77	0.84	1.07 (0.56–2.04)

CI, confidence interval; CNV, choroidal neovascularization; HM, high myopia; HWE, Hardy–Weinberg equilibrium; OR, odds ratio; SNP, single nucleotide polymorphism.
[a]The repeatedly replicated AMD-risk allele is allele A in rs11200638, allele T in rs10490924, and C in rs1061170, respectively.
[b]Hardy–Weinberg equilibrium for the genotypic distribution was examined using the HWE-exact test.
[c]Differences in the observed genotypic distribution was examined by the Trend χ^2 test.
[d]Age, gender adjustment was performed based on a logistic regression model by assuming an additive effect in each of the three SNPs.

Table 3 Association of inferred haplotype for rs10490924—rs11200638 with CNV in highly myopic eyes of the elderly Japanese population in this study

Haplotype	*Haplotype frequency*	*Frequencies in case and control*		P-*value*[a]	
		HM-CNV group (n = 183)	*HM-control group* (n = 170)	*Nominal*	*Corrected*
G-G	0.611	0.587	0.623	0.32	0.71
T-A	0.365	0.409	0.356	0.14	0.39
G-A	0.017	0.004	0.021	0.04	0.10

CNV, choroidal neovascularization; HM, high myopia.
[a]The nominal *P*-values were calculated by the χ^2 test, and multiple testing correction for the *P*-value was performed by the permutation test (number of iterations = 10000).

gender and age differences based on a logistic regression model by assuming an additive effect of each of the three SNPs, no new significant differences were found between the two groups. We performed a subset analysis on the 141 highly myopic cases with monocular CNV. Again, no significant differences were found in the genotypic distribution for these subjects (data not shown). To examine the effects of different age inclusion criteria, we also performed subset analyses on much older HM-CNV and HM control (≥55, ≥60, and ≥65 years of age). However, no new significant differences were found in this study (data not shown).

In this study population, rs11200638 and rs10490924 were in strong LD (D′ = 0.97). The inferred haplotype frequencies in the HM-CNV group and the HM-control group are shown in Table 3. The haplotype frequencies were not significantly different between the HM-CNV group and the HM-control group after the multiple testing corrections. Haplotype analyses using the subset of cases with monocular CNV also did not show any significant differences even before the multiple testing correction (data not shown).

Single SNP analyses and haplotype analyses between the HM-CNV group and PB-control group for the three SNPs also showed no significant associations (data not shown).

We analysed the genotypic distributions for rs10490924, rs11200638, and rs1061170 in the pooled highly myopic cases (HM-CNV group + HM-control group) and compared them with the PB-control group to check for a possible difference in the genetic background for the three AMD-associated SNPs in the highly myopic population. The results are shown in Table 4. The distributions of the genotypes were all in HWE ($P > 0.1$). There were no significant differences even after gender and age adjustment between the pooled highly myopic cases and the PB-control group.

Discussion

The results of this study showed that the genotypic distribution of three AMD-associated SNPs, rs11200638, rs10490924 and rs1061170, in highly myopic elderly Japanese patients with CNV did not differ significantly from that in highly myopic elderly Japanese without CNV. All of the highly myopic patients with binocular CNV in our study had an old CNV in the fellow eye at their first visit, suggesting that some of the patients

Table 4 Genotype counts, associations, and odds ratios for rs10490924, rs11200638, and rs1061170 in the pooled high myopia group and the population-based control group

SNP	*Geotype*[a]	*Pooled HM group* (n = 353)		*PB-control group* (n = 374)		P^c	*Age and gender adjusted*[d]	
		Genotype count	*HWE* P^b	*Genotype count*	*HWE* P^b		*P*	*OR (95% CI)*
rs10490924 ARMS2 Ala69Ser	GG/GT/TT	133/164/51	1.00	151/174/46	0.74	0.35	0.48	0.82 (0.47–1.43)
rs11200638 HTRA1(−625G > A)	GG/GA/AA	124/171/54	0.74	147/163/53	0.50	0.26	0.36	0.78 (0.45–1.33)
rs1061170 CFH Tyr402His	TT/TC/CC	306/38/1	1.00	313/58/0	0.15	0.12	0.21	0.48 (0.15–1.54)

CI, confidence interval; CNV, choroidal neovascularization; HM, high myopia; HWE, Hardy–Weinberg equilibrium; OR, odds ratio; PB, population-based; SNP, single nucleotide polymorphism.
[a]The repeatedly replicated AMD-risk allele is allele A in rs11200638, allele T in rs10490924, and C in rs1061170, respectively.
[b]Hardy–Weinberg equilibrium for the genotypic distribution was examined using the HWE-exact test.
[c]Differences in the observed genotypic distribution was examined by the Trend χ^2 test.
[d]Age, gender-adjustment was performed based on a logistic regression model by assuming an additive effect in each of the three SNPs.

might have had a CNV long before their first visit, that is they might have had a CNV before reaching 50 years of age. Thus, we analysed a subset of the HM-CNV group with monocular CNV, but still no significant differences were found in the distribution of the three SNPs. These results indicated that the molecular or cellular events that are related to these AMD-associated SNPs have little, or small if any, contribution to the development of CNV in highly myopic eyes of the elderly Japanese population.

CNV is a complication common to both high myopia and AMD.[3] It can be difficult or impossible to distinguish between the CNV that is attributable to excessive axial elongation and the CNV that is attributable to the aetiology of the wet-type AMD in highly myopic eyes of the elderly.[1] The important phenotypic hallmarks of AMD are soft drusen and pigment abnormalities in the macular area.[38–40] In the highly myopic eyes of elderly patients, other characteristic changes typical of pathological myopia, for example chorioretinal atrophy, lacquer cracks, or posterior staphyloma, are often present.[41] These degenerative changes make it difficult to determine, using ophthalmoscopic examinations, whether the hallmarks of AMD are present. Thus, we hypothesized that highly myopic patients who develop CNV after 50 years of age may have some contribution from the same genetic factors associated with AMD.

Recently, Fernandez-Robredo *et al*[34] investigated a possible contribution of the two AMD-associated SNPs, rs1061170 (Y402H) and rs10490924 (A69S), to CNV associated with high myopia in a Spanish population >30 years of age. This group studied 100 patients with CNV associated with high myopia and 96 age-matched highly myopic controls without CNV. They did not find a significant difference in the genotypic distribution between the two groups for these AMD-associated SNPs. In this study, we focused on more elderly patients, that is ⩾50 years of age, with CNV in highly myopic eyes to maximize the detection power based on the hypothesis that the contribution by these AMD-associated SNPs to the development of CNV may be stronger in older patients. Our study in elderly myopic patients (183 HM-CNV cases and 170 HM controls) has an 80% power at an α-error of 0.05 for detection of an OR >1.88 when the risk allele frequency is 0.35 in the controls (rs10490924 and rs11200638) and an OR >3.19 when the control risk allele frequency is 0.05 (rs1061170). However, we did not find any significant differences.

Some case–control studies in the elderly and population-based epidemiological studies have reported that hypermetropia is one of the risk factors for early age-related maculopathy (early ARM) and/or late ARM (ie AMD).[42–48] From the results of the Beijing Eye Study, Xu *et al*[49] reported that the prevalence of both early and late ARM was significantly lower in the highly myopic group. We also analysed the differences in the genotypic distributions for the AMD-associated SNPs by the Trend χ^2 test between the pooled elderly (⩾50 years old) highly myopic cases (HM-CNV group + HM-control group) and the PB-control group. The difference between the two groups was not significant. Although the recruitment of the highly myopic cases in our study was not population –based, but hospital based, these results suggest that the low prevalence of AMD in highly myopic cases cannot be explained simply by the difference of genetic background on the AMD-associated locus between highly myopic cases and the general population.

This study has some limitations. First, the age of the HM-CNV patients was recorded at the first visit. We did not know the exact time of the onset of the CNV, and there might have been an interval between the development of CNV and the examinations in some cases. This possibility is important in the cases with binocular CNV at their first consultation because old CNV was present in their fellow eyes. To reduce this bias, we performed a subset analysis on monocular CNV cases only. However, the results did not change. Second, the HM-CNV group and HM-control group were not age and gender matched. To minimize the possible influence

of these differences, we performed age and gender adjustments using the logistic regression analysis and found no new significant associations. Third, the age range of the population-based control group in this study was significantly younger than that in the high myopia groups. Some of these young controls may develop axial elongation and may become 'highly myopic' in the future. Therefore, the case–control association analyses using these subjects tend to be statistically conservative. To circumvent the shortcomings, it will be important to perform a replication analysis using age-matched population-based controls.

In summary, our results show that the genotypic distribution of three AMD-associated SNPs (rs10490924 (A69S) of *ARMS2/LOC387715*, rs11200638 of *HTRA1*, and rs1061170 (Y402H) of *CFH*) in highly myopic elderly Japanese patients with CNV was not significantly different from that in highly myopic Japanese patients without CNV. These results indicate that these SNPs do not contribute significantly to the development of CNV in highly myopic eyes of the elderly Japanese population.

Conflict of interest

The authors declare no conflict of interest.

Acknowledgements

The study was supported in part by the Ministry of Education, Culture, Sports, Science ,and Technology of Japan and by the Japanese National Society for the Prevention of Blindness.

References

1 Soubrane G. Choroidal neovascularization in pathologic myopia: recent developments in diagnosis and treatment. *Surv Ophthalmol* 2008; **53**: 121–138.
2 Ohno-Matsui K, Yoshida T, Futagami S, Yasuzumi K, Shimada N, Kojima A *et al*. Patchy atrophy and lacquer cracks predispose to the development of choroidal neovascularisation in pathological myopia. *Br J Ophthalmol* 2003; **87**: 570–573.
3 Grossniklaus HE, Green WR. Choroidal neovascularization. *Am J Ophthalmol* 2004; **137**: 496–503.
4 Cohen SY, Laroche A, Leguen Y, Soubrane G, Coscas GJ. Etiology of choroidal neovascularization in young patients. *Ophthalmology* 1996; **103**: 1241–1244.
5 Haddad S, Chen CA, Santangelo SL, Seddon JM. The genetics of age-related macular degeneration: a review of progress to date. *Surv Ophthalmol* 2006; **51**: 316–363.
6 Gorin MB. A clinician's view of the molecular genetics of age-related maculopathy. *Arch Ophthalmol* 2007; **125**: 21–29.
7 Swaroop A, Branham KE, Chen W, Abecasis G. Genetic susceptibility to age-related macular degeneration: a paradigm for dissecting complex disease traits. *Hum Mol Genet* 2007; **16**(Spec No. 2): R174–R182.
8 Edwards AO, Ritter 3rd R, Abel KJ, Manning A, Panhuysen C, Farrer LA. Complement factor H polymorphism and age-related macular degeneration. *Science* 2005; **308**: 421–424.
9 Hageman GS, Anderson DH, Johnson LV, Hancox LS, Taiber AJ, Hardisty LI *et al*. A common haplotype in the complement regulatory gene factor H (HF1/CFH) predisposes individuals to age-related macular degeneration. *Proc Natl Acad Sci USA* 2005; **102**: 7227–7232.
10 Haines JL, Hauser MA, Schmidt S, Scott WK, Olson LM, Gallins P *et al*. Complement factor H variant increases the risk of age-related macular degeneration. *Science* 2005; **308**: 419–421.
11 Klein RJ, Zeiss C, Chew EY, Tsai JY, Sackler RS, Haynes C *et al*. Complement factor H polymorphism in age-related macular degeneration. *Science* 2005; **308**: 385–389.
12 Zareparsi S, Branham KE, Li M, Shah S, Klein RJ, Ott J *et al*. Strong association of the Y402H variant in complement factor H at 1q32 with susceptibility to age-related macular degeneration. *Am J Hum Genet* 2005; **77**: 149–153.
13 Baird PN, Islam FM, Richardson AJ, Cain M, Hunt N, Guymer R. Analysis of the Y402H variant of the complement factor H gene in age-related macular degeneration. *Invest Ophthalmol Vis Sci* 2006; **47**: 4194–4198.
14 Conley YP, Jakobsdottir J, Mah T, Weeks DE, Klein R, Kuller L *et al*. CFH, ELOVL4, PLEKHA1 and LOC387715 genes and susceptibility to age-related maculopathy: AREDS and CHS cohorts and meta-analyses. *Hum Mol Genet* 2006; **15**: 3206–3218.
15 Lau LI, Chen SJ, Cheng CY, Yen MY, Lee FL, Lin MW *et al*. Association of the Y402H polymorphism in complement factor H gene and neovascular age-related macular degeneration in Chinese patients. *Invest Ophthalmol Vis Sci* 2006; **47**: 3242–3246.
16 Magnusson KP, Duan S, Sigurdsson H, Petursson H, Yang Z, Zhao Y *et al*. CFH Y402H confers similar risk of soft drusen and both forms of advanced AMD. *PLoS Med* 2006; **3**: e5.
17 Maller J, George S, Purcell S, Fagerness J, Altshuler D, Daly MJ *et al*. Common variation in three genes, including a noncoding variant in CFH, strongly influences risk of age-related macular degeneration. *Nat Genet* 2006; **38**: 1055–1059.
18 Postel EA, Agarwal A, Caldwell J, Gallins P, Toth C, Schmidt S *et al*. Complement factor H increases risk for atrophic age-related macular degeneration. *Ophthalmology* 2006; **113**: 1504–1507.
19 Seddon JM, Francis PJ, George S, Schultz DW, Rosner B, Klein ML. Association of CFH Y402H and LOC387715 A69S with progression of age-related macular degeneration. *JAMA* 2007; **297**: 1793–1800.
20 Jakobsdottir J, Conley YP, Weeks DE, Mah TS, Ferrell RE, Gorin MB. Susceptibility genes for age-related maculopathy on chromosome 10q26. *Am J Hum Genet* 2005; **77**: 389–407.
21 Rivera A, Fisher SA, Fritsche LG, Keilhauer CN, Lichtner P, Meitinger T *et al*. Hypothetical LOC387715 is a second major susceptibility gene for age-related macular degeneration, contributing independently of complement factor H to disease risk. *Hum Mol Genet* 2005; **14**: 3227–3236.
22 Dewan A, Liu M, Hartman S, Zhang SS, Liu DT, Zhao C *et al*. HTRA1 promoter polymorphism in wet age-related macular degeneration. *Science* 2006; **314**: 989–992.
23 Yang Z, Camp NJ, Sun H, Tong Z, Gibbs D, Cameron DJ *et al*. A variant of the HTRA1 gene increases susceptibility to age-related macular degeneration. *Science* 2006; **314**: 992–993.

24 Cameron DJ, Yang Z, Gibbs D, Chen H, Kaminoh Y, Jorgensen A *et al*. HTRA1 variant confers similar risks to geographic atrophy and neovascular age-related macular degeneration. *Cell Cycle* 2007; **6**: 1122–1125.
25 Fisher SA, Rivera A, Fritsche LG, Babadjanova G, Petrov S, Weber BH. Assessment of the contribution of CFH and chromosome 10q26 AMD susceptibility loci in a Russian population isolate. *Br J Ophthalmol* 2007; **91**: 576–578.
26 Kanda A, Chen W, Othman M, Branham KE, Brooks M, Khanna R *et al*. A variant of mitochondrial protein LOC387715/ARMS2, not HTRA1, is strongly associated with age-related macular degeneration. *Proc Natl Acad Sci USA* 2007; **104**: 16227–16232.
27 Kondo N, Honda S, Ishibashi K, Tsukahara Y, Negi A. LOC387715/HTRA1 variants in polypoidal choroidal vasculopathy and age-related macular degeneration in a Japanese population. *Am J Ophthalmol* 2007; **144**: 608–612.
28 Leveziel N, Souied EH, Richard F, Barbu V, Zourdani A, Morineau G *et al*. PLEKHA1-LOC387715-HTRA1 polymorphisms and exudative age-related macular degeneration in the French population. *Mol Vis* 2007; **13**: 2153–2159.
29 Lu F, Hu J, Zhao P, Lin Y, Yang Y, Liu X *et al*. HTRA1 variant increases risk to neovascular age-related macular degeneration in Chinese population. *Vision Res* 2007; **47**: 3120–3123.
30 Mori K, Horie-Inoue K, Kohda M, Kawasaki I, Gehlbach PL, Awata T *et al*. Association of the HTRA1 gene variant with age-related macular degeneration in the Japanese population. *J Hum Genet* 2007; **52**: 636–641.
31 Ross RJ, Bojanowski CM, Wang JJ, Chew EY, Rochtchina E, Ferris 3rd FL *et al*. The LOC387715 polymorphism and age-related macular degeneration: replication in three case-control samples. *Invest Ophthalmol Vis Sci* 2007; **48**: 1128–1132.
32 Tanimoto S, Tamura H, Ue T, Yamane K, Maruyama H, Kawakami H *et al*. A polymorphism of LOC387715 gene is associated with age-related macular degeneration in the Japanese population. *Neurosci Lett* 2007; **414**: 71–74.
33 Yoshida T, DeWan A, Zhang H, Sakamoto R, Okamoto H, Minami M *et al*. HTRA1 promoter polymorphism predisposes Japanese to age-related macular degeneration. *Mol Vis* 2007; **13**: 545–548.
34 Fernandez-Robredo P, Maestre SR, Zarranz-Ventura J, Mulero HH, Salinas-Alaman A, Garcia-Layana A. Myopic choroidal neovascularization genetics. *Ophthalmology* 2008; **115**: 1632, 1632 e1.
35 Gushima H. Pharma SNP Consortium (PSC). Research on Pharmacokinetics related Genetic Polymorphism among Japanese Population. *Xenobiotic Metab and Dispos* 2001; **16**: 340–345.
36 Pesarin F. *Multivariate Permutation Tests: With Applications in Biostatistics*. Wiley-Blackwell: Chichester, UK, 2001.
37 Barrett JC, Fry B, Maller J, Daly MJ. Haploview: analysis and visualization of LD and haplotype maps. *Bioinformatics* 2005; **21**: 263–265.
38 Bird AC, Bressler NM, Bressler SB, Chisholm IH, Coscas G, Davis MD *et al*. An international classification and grading system for age-related maculopathy and age-related macular degeneration. The International ARM Epidemiological Study Group. *Surv Ophthalmol* 1995; **39**: 367–374.
39 Age-Related Eye Disease Study Research Group. The Age-Related Eye Disease Study system for classifying age-related macular degeneration from stereoscopic color fundus photographs: the Age-Related Eye Disease Study Report Number 6. *Am J Ophthalmol* 2001; **132**: 668–681.
40 Klein R, Peto T, Bird A, Vannewkirk MR. The epidemiology of age-related macular degeneration. *Am J Ophthalmol* 2004; **137**: 486–495.
41 Curtin BJ, Karlin DB. Axial length measurements and fundus changes of the myopic eye. I. The posterior fundus. *Trans Am Ophthalmol Soc* 1970; **68**: 312–334.
42 The Eye Disease Case-Control Study Group. Risk factors for neovascular age-related macular degeneration. *Arch Ophthalmol* 1992; **110**: 1701–1708.
43 Sandberg MA, Tolentino MJ, Miller S, Berson EL, Gaudio AR. Hyperopia and neovascularization in age-related macular degeneration. *Ophthalmology* 1993; **100**: 1009–1013.
44 Chaine G, Hullo A, Sahel J, Soubrane G, Espinasse-Berrod MA, Schutz D *et al*. Case-control study of the risk factors for age related macular degeneration. France-DMLA Study Group. *Br J Ophthalmol* 1998; **82**: 996–1002.
45 Wang JJ, Mitchell P, Smith W. Refractive error and age-related maculopathy: the Blue Mountains Eye Study. *Invest Ophthalmol Vis Sci* 1998; **39**: 2167–2171.
46 Age-Related Eye Disease Study Research Group. Risk factors associated with age-related macular degeneration. A case-control study in the age-related eye disease study: Age-Related Eye Disease Study Report Number 3. *Ophthalmology* 2000; **107**: 2224–2232.
47 Ikram MK, van Leeuwen R, Vingerling JR, Hofman A, de Jong PT. Relationship between refraction and prevalent as well as incident age-related maculopathy: the Rotterdam Study. *Invest Ophthalmol Vis Sci* 2003; **44**: 3778–3782.
48 Xu L, Li Y, Zheng Y, Jonas JB. Associated factors for age related maculopathy in the adult population in China: the Beijing eye study. *Br J Ophthalmol* 2006; **90**: 1087–1090.
49 Xu L, Li Y, Wang S, Wang Y, Wang Y, Jonas JB. Characteristics of highly myopic eyes: the Beijing Eye Study. *Ophthalmology* 2007; **114**: 121–126.

MAJOR ARTICLE

Genomewide Association Study of a Rapid Progression Cohort Identifies New Susceptibility Alleles for AIDS (ANRS Genomewide Association Study 03)

Sigrid Le Clerc,[1,2,4,a] Sophie Limou,[1,2,4,5,a] Cédric Coulonges,[1,2] Wassila Carpentier,[2] Christian Dina,[6] Lieng Taing,[1] Olivier Delaneau,[1] Taoufik Labib,[1,4] Rob Sladek,[8] ANRS Genomic Group,[2,b] Christiane Deveau,[2] Hélène Guillemain,[1] Rojo Ratsimandresey,[1] Matthieu Montes,[1] Jean-Louis Spadoni,[1] Amu Therwath,[3] François Schächter,[1] Fumihiko Matsuda,[9] Ivo Gut,[5] Jean-Daniel Lelièvre,[4] Yves Lévy,[4] Philippe Froguel,[6,10] Jean-François Delfraissy,[2] Serge Hercberg,[7] and Jean-François Zagury[1,2,4]

[1]Chaire de Bioinformatique, Conservatoire National des Arts et Métiers, [2]Agence Nationale de Recherche sur le SIDA (ANRS) Genomic Group, and [3]Laboratoire d'Oncologie Moléculaire, Paris, and [4]Université Paris 12, Institut National de la Santé et de la Recherche Médicale (INSERM) U955, Créteil, [5]Commissariat à L'Energie Atomique/Institut de Génomique, Centre National de Génotypage, Evry, [6]Unité Mixte de Recherche (UMR) Centre National de la Recherche Scientifique 8090, Institut Pasteur de Lille, Lille Cedex, and [7]UMR U557 INSERM/U1125 Institut National de la Recherche Agronomique/Conservatoire National des Arts et Métiers/Université Paris 13, and Centre de Recherche en Nutrition Humaine Ile-de-France, Santé-Médecine-Biologie Humaine (SMBH) Paris 13, Bobigny, France; [8]Department of Human Genetics, Faculty of Medicine, McGill University, and Génome Québec Innovation Centre, Montreal, Canada; [9]INSERM U852, Center for Genomic Medicine, Kyoto University Graduate School of Medicine, Kyoto, Japan; [10]Genomic Medicine, Hammersmith Hospital, Imperial College London, London, United Kingdom

Background. Previous genomewide association studies (GWASs) of AIDS have targeted end points based on the control of viral load and disease nonprogression. The discovery of genetic factors that predispose individuals to rapid progression to AIDS should also reveal new insights into the molecular etiology of the pathology.

Methods. We undertook a case-control GWAS of a unique cohort of 85 human immunodeficiency virus type 1 (HIV-1)–infected patients who experienced rapid disease progression, using Illumina HumanHap300 BeadChips. The case group was compared with a control group of 1352 individuals for the 291,119 autosomal single-nucleotide polymorphisms (SNPs) passing the quality control tests, using the false-discovery rate (FDR) statistical method for multitest correction.

Results. Novel associations with rapid progression (FDR, ≤25%) were identified for *PRMT6* ($P = 6.1 \times 10^{-7}$; odds ratio [OR], 0.24), *SOX5* ($P = 1.8 \times 10^{-6}$; OR, 0.45), *RXRG* ($P = 3.9 \times 10^{-6}$; OR, 3.29), and *TGFBRAP1* ($P = 7 \times 10^{-6}$; OR, 0.34). The haplotype analysis identified exonic and promoter SNPs potentially important for *PRMT6* and *TGFBRAP1* function.

Conclusions. The statistical and biological relevance of these associations and their high ORs underscore the power of extreme phenotypes for GWASs, even with a modest sample size. These genetic results emphasize the role of the transforming growth factor β pathway in the pathogenesis of HIV-1 disease. Finally, the wealth of information provided by this study should help unravel new diagnostic and therapeutic targets.

Genomewide association studies (GWASs) may provide new insights into the molecular etiology of complex diseases by discovering unsuspected genetic risk factors and, as a consequence, identify new diagnostic or therapeutic targets [1]. Reports of 3 GWASs of AIDS have already been published [2–4] and described mainly

Received 8 April 2009; accepted 28 May 2009; electronically published 15 September 2009.

Reprints or correspondence: Dr Jean-François Zagury, Conservatoire National des Arts et Métiers, 292 rue Saint Martin, 75003 Paris, France (zagury@cnam.fr).

The Journal of Infectious Diseases 2009;200:1194–201

0022-1899/2009/20008-0003$15.00
DOI: 10.1086/605892

Potential conflicts of interest: none reported.

Financial support: Agence Nationale de Recherche sur le SIDA (ANRS); Innovation 2007 program of Conservatoire National des Arts et Métiers; AIDS Cancer Vaccine Development Foundation; Neovacs SA; Vaxconsulting. S.L. benefits from a fellowship from the French Ministry of Education, Technology, and Research, and S.L.C. benefits from a fellowship from the ANRS.

[a] S.L.C. and S.L. contributed equally to this work.

[b] The ANRS Genomic Group oversees the AIDS genomic projects of the ANRS; study group members are listed at the end of the text.